ELSEVIER

Journal of Structural Geology 27 (2005) 964–984

JOURNAL OF STRUCTURAL GEOLOGY

www.elsevier.com/locate/jsg

# Geophysical testing of balanced cross-sections of fold–thrust belts with potential field data: an example from the Fleurieu Arc of the Delamerian Orogen, South Australia

N.G. Direen*, D. Brock, M. Hand

*Continental Evolution Research Group, School of Earth and Environmental Sciences, University of Adelaide, Adelaide, SA 5005, Australia*

Received 6 September 2004; received in revised form 5 March 2005; accepted 14 March 2005
Available online 13 June 2005

**Abstract**

The Delamerian (South Australia) and Ross (Antarctica) Orogens once formed a continuous chain along the paleo-Pacific margin of Gondwana. Correlations between the two are based on many characteristics, including style of shortening and deformation. Constraining structural features in one of these orogens impacts on interpretations of tectonic processes for the other. Balanced cross-sections have provided crucial information on the internal architecture of the Delamerian Orogen, South Australia, and form a key piece of evidence in some widely circulated models for the deformational style. These sections have not been constrained by geophysical investigations, which can provide significant information about the subsurface geometry.

We present magnetic forward models for two balanced cross-sections of the Fleurieu Arc in the Delamerian Orogen. The forward models require a larger volume of magnetic basement at shallower depths than predicted by balanced sections, requiring a revision of currently proposed shortening mechanisms. The shortening mechanism inferred from the models requires less imbrication of upper crustal units, and more folding above thrusts that involve both basement and cover sequences. This style of shortening compares favorably with published observations from the Ross Orogen in Antarctica.


*Keywords:* Balanced cross-sections; Fleurieu Arc; Foreland fold–thrust belt; Magnetic modeling; Ross–Delamerian Orogen; South Australia

## 1. Introduction

There are three classes of tests for evaluating the validity of balanced cross-sections within thrust belts: geometrical, mechanical and geophysical (De Paor, 1988). Much of the existing literature on balanced sections deals with the first two of these criteria (Dahlstrom, 1969; Elliott, 1983; De Paor, 1988; Jones, 1988; Rowan and Kligfield, 1989; Woodward et al., 1989; Mitra, 2002); however, there are relatively fewer studies dealing with the latter. Of these, the majority deal principally with the integration of seismic reflection constraints (Gibbs, 1983; Morgan and Karig, 1995; Hardage et al., 1999; Power et al., 2001) as a means of testing the viability and admissibility of balanced sections geophysically, or of balancing to test admissibility of seismic interpretations.

Seismic reflection data are typically expensive to acquire, and often face logistical and acquisition difficulties within typical fold–thrust-belt sequences, due to rugged terrane (Foster et al., 1998), structures with steep dips (Jones and Johnstone, 2001), lithological and tectonic complexity (Dutta and Chatterjee, 1998), or combinations of these factors. Expense alone tends to limit the use of seismic reflection data in geophysically testing viability of balanced sections, and seismic acquisition is usually restricted to areas of specific economic interest, such as where hydrocarbons are proven or suspected (Dutta and Chatterjee, 1998; Hardage et al., 1999). Thus, many examples of fold-and-thrust belts that have no hydrocarbon potential also have little or no opportunity to test and validate shortening models using seismic reflection data. Other methods for the geophysical validation of balanced sections, as suggested by De Paor (1988), must therefore be employed.

Regional gravity and magnetic data are often routinely

* Corresponding author. Tel.: +61 8 83035841; fax: +61 8 83034347.
*E-mail address:* nick.direen@adelaide.edu.au (N.G. Direen).

0191-8141/$ - see front matter © 2005 Elsevier Ltd. All rights reserved.
doi:10.1016/j.jsg.2005.03.004

and cheaply acquired in many foldbelts, which remain otherwise untested by seismic reflection data. Gravity and magnetics can be used to make interpretations of structure in blind basement areas or in difficult terrain, and can be readily combined with structural observations from drilling or outcrops (Direen and Lyons, 2002; Betts et al., 2003; McLean and Betts, 2003).

If the magnetic susceptibility and density properties of the foldbelt stratigraphy are known or can be estimated (Betts et al., 2003; McLean and Betts, 2003), gravity and magnetic field data can also be used to test the admissibility of cross-section geometries constructed from sparse field structural data using forward modeling techniques (Jessell and Valenta, 1996). Properties such as the geometry of faults and shear zones, including their dips and directions at depth (Paul et al., 1966; Direen and Leaman, 1997; Direen, 1998), and depth, size and shape of igneous intrusions (Ameglio and Vigneresse, 1999) and sedimentary sequences (Sayers et al., 2001) can all be constrained, providing key information on disposition of restorable units at depth.

Because of the relative ubiquity of high-quality gravity and magnetic datasets, and the relative ease with which field geologists can acquire relevant rock property information, it is now possible to test the predictions of balanced cross-sections in many places around the world, even in the absence of seismic reflection data. Here we present one such example.

Situated in southeastern Australia (Fig. 1), the Fleurieu Arc (see Marshak and Flöttmann (1996) for definitions of this terminology) of the Ross–Delamerian Orogen (Flöttmann and Oliver, 1994) is a well-exposed, well-developed example of an early Paleozoic (Middle Cambrian–Early Ordovician) foreland fold-and-thrust belt (Jenkins and Sandiford, 1992). Jenkins (1990) and Flöttmann and co-workers (Flöttmann et al., 1994, 1995, 1998; Marshak and Flöttmann, 1996; Flöttmann and James, 1997; Yassaghi et al., 2000, 2004) have recognized and described a significant foreland zone of craton-vergent thrusting within this fold belt.

The Ross–Delamerian Orogen is important globally, as it is the first expression of a broad change in tectonic regime at the Gondwana continental margin from a trailing margin, to convergent subduction tectonics (Foden et al., 2002). Compression resulted in accretion of outboard, arc-related terranes to both Australia and Antarctica (e.g. Crawford et al., 2003). Initiation of the Ross Orogen is somewhat earlier (~544 Ma: Black and Sheraton, 1990; Goodge et al., 1991, 1993) than the Delamerian, which is bracketed by ages of late sedimentation (Cooper et al., 1992) and orogenic intrusions to ~514–485 Ma (Foden et al., 2002).

The continuity of the Australia and Antarctica as neighboring blocks within Gondwana is now well accepted (Stump et al., 1986; Storey et al., 1996). This correlation is based on similarities between the late Archean–early Proterozoic cratonic geology (Oliver et al., 1983; Sheraton et al., 1993; Peucat et al., 1999) and the similarities of the bordering Paleozoic mobile belts (Flöttmann et al., 1993a,b). The lithological character of deformed basins and accreted terranes, along with patterns of magmatism and metamorphism, are important aspects in comparisons. However, the styles and timing of deformation are the most broadly applied and persuasive criteria for linking the Ross (Antarctica) and Delamerian (South Australia) Orogens (Flöttmann et al., 1993a,b). Therefore, any reappraisal of deformational style on one continental block has important consequences for correlations with the other.

Crucial to the arguments regarding the structural style and degree of shortening in the Ross–Delamerian Orogen has been the use of balanced and restorable cross-sections (Marshak and Woodward, 1988), which invoke basement-involved blind thrusts and cover–basement detachments (Flöttmann et al., 1994, 1995; Marshak and Flöttmann, 1996; Flöttmann and James, 1997). These models for the deformation of the Fleurieu Arc place important constraints on the evolution of the evolving Gondwanide passive margin in eastern Gondwana, during the Ross–Delamerian Orogeny (Flöttmann and Kleinschmidt, 1991; Flöttmann et al., 1993a).

Because geometric and mechanical models for the Fleurieu Arc are now relatively advanced, and because this foldbelt is well covered by high quality regional aeromagnetic datasets, it forms an ideal natural laboratory in which to demonstrate some simple but effective tests of balanced cross-sections, where no seismic reflection data currently exists. In this paper, we present new constraints on models for the internal architecture of the Fleurieu Arc, using measured apparent magnetic susceptibility from the exposed rocks and structures, and the geometric constraints imparted by two mechanically/geometrically admissible sections of Flöttmann et al. (1994). We use both geophysical forward models and inversions of the observed magnetic field to constrain positions of blind basement blocks involved in thick-skinned thrusting. We then discuss the implications of this data on models for shortening within the wider Ross–Delamerian orogenic system.

## 2. Regional geology

The Ross–Delamerian Orogen formed along the paleo-Pacific margin of Gondwana during the Late Cambrian to Early Ordovician (ca. 514–485 Ma) (Foden et al., 2002). The Delamerian Orogeny metamorphosed and deformed Neoproterozoic and Cambrian rift- and sag-basin sediments (Von Der Borch, 1980; Preiss, 1987, 2000; Powell et al., 1994), causing basin inversion (Yassaghi et al., 2000, 2004) with some involvement of the Paleo- to Mesoproterozoic basement (Flöttmann et al., 1994; Preiss, 2000).

### 2.1. Regional stratigraphy

The Paleozoic and Proterozoic rocks of the Fleurieu Arc

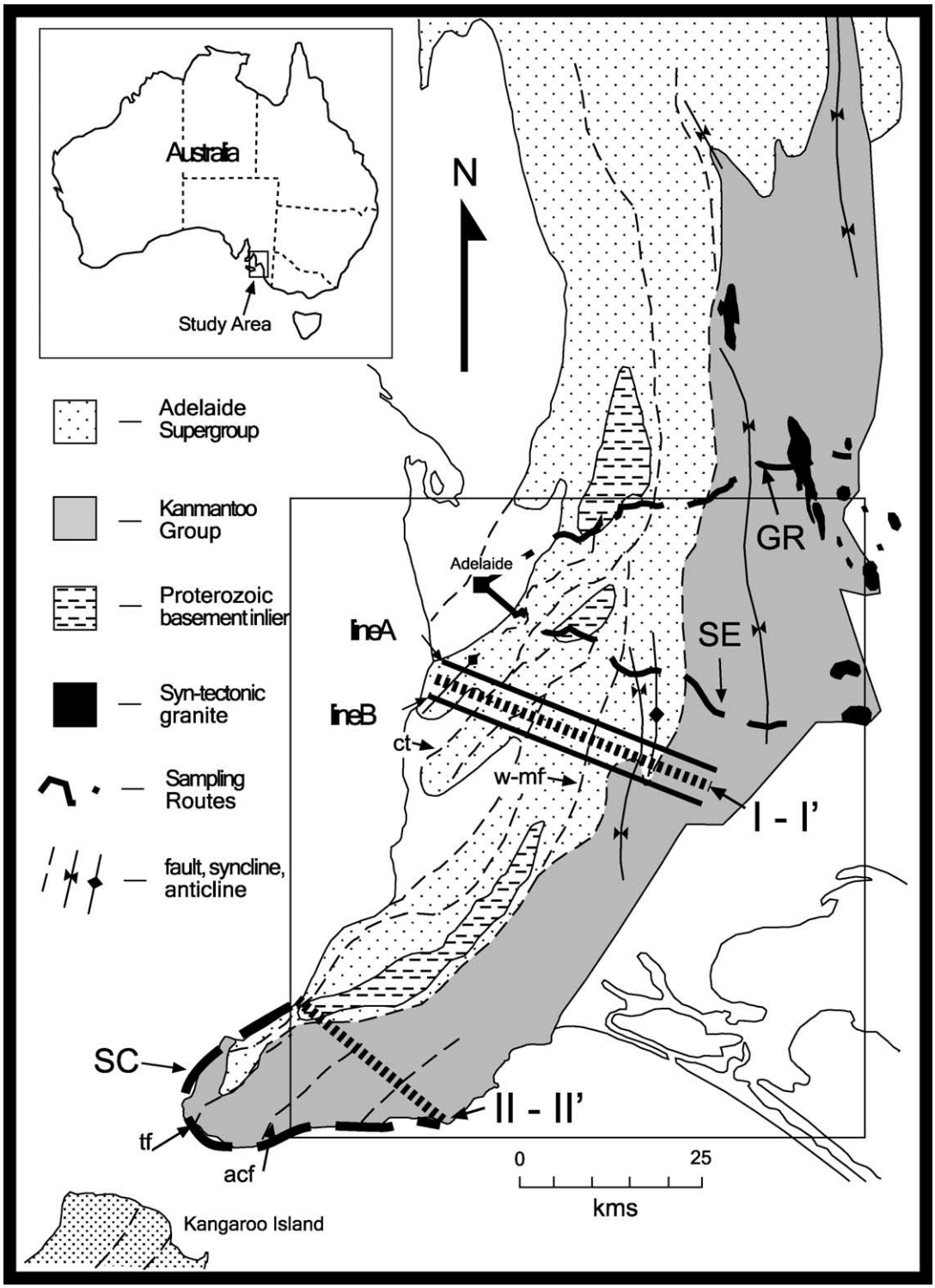


Fig. 1. Regional geological map of the southern Adelaide Fold Belt showing ~N–S trends of major structures (modified from Preiss (1995a,b)). The sampling routes are shown by large dashed lines. I–I′ and II–II′ indicate the transects restored by Flöttmann et al. (1994) as balanced cross-sections. Lines 'A', 'B' and II–II′ are the lines extracted from the TMI dataset for geophysical forward modeling (Fig. 4) and the thin, solid line box is area shown in Fig. 4 (SE = southern sampling route, GR = northern sampling route, SC = coastal sampling route; ct = Clarendon Thrust, w–mf = Williamstown–Meadows Fault, tf = Talisker Fault, acf = Aaron Creek Fault).

have been subdivided by Preiss (1987). The crystalline basement is exposed in a series of four inliers (Figs. 1 and 2), from north to south, the Houghton, Aldgate, Myponga and Normanville inliers. These inliers—collectively termed the Barossa Complex—comprise a diverse array of deformed rock types, including hydrothermally altered schists, gneisses, pegmatites, phyllonites, and felsic and mafic intrusives, believed to be Proterozoic in age (Belperio et al., 1998). Flöttmann et al. (1994) and Flöttmann and James (1997) correlated the Barossa Complex with the Archean–Proterozoic Gawler Craton, which lies to the west and northwest of the Fleurieu Arc.

Overlying the Barossa Complex with pronounced regional unconformity are sedimentary rocks of the Late Proterozoic Adelaide Rift Complex (Preiss, 1987). The lowermost unit of the rift is the Warrina Supergroup, comprising the lower Callana Group, and the upper Burra Group. The Callana Group is not represented in our study area, and will not be considered further. The Burra Group comprises a number of units. Of importance in this study

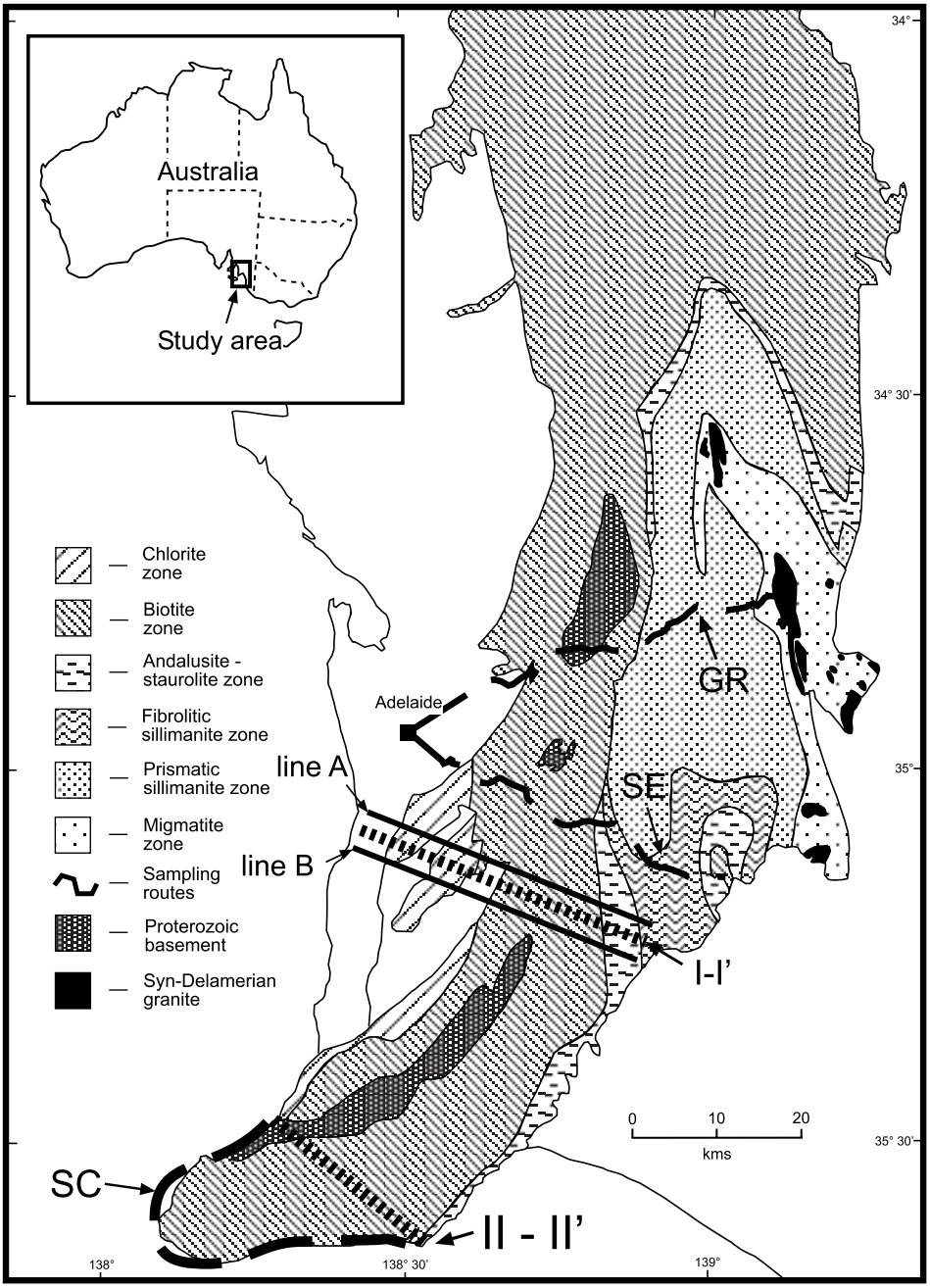


Fig. 2. Metamorphic isograds of the southern Delamerian Orogen as defined by 'mineral-in' boundaries (modified from Offler and Fleming (1968) and Preiss (1995a,b)). Overlays are the same as for Fig. 1.

were those sequences used by Flöttmann et al. (1994) to create their balanced cross-sections; these are principally competent marker horizons that have evidence for minimal internal strains, separated by thicker incompetent packages (Flöttmann and James, 1997). Marker units in the Burra Group include the lowermost Aldgate Sandstone, a distinctive siliceous conglomeratic unit; the thin Skillogallee Dolomite; the Woolshed Flat Shale; the Stonyfell Quartzite; the pelitic Saddleworth Formation; and interbedded slate and quartzite of the Belair Subgroup (Fig. 3).

The Warrina Supergroup is unconformably overlain by the Umberatana Group and Wilpena Group, which together form the Heysen Supergroup (Preiss, 1987). Balancing units within the former include the Sturt Tillite at the base and the Tapley Hill Formation. The main balancing unit in the Wilpena Group is the Ulupa Siltstone (Fig. 3).

The lower Paleozoic Moralana Supergroup sits unconformably above the Heysen Supergroup in the Fleurieu Arc. It comprises the lower Normanville Group and the upper Kanmantoo Group. The Normanville Group comprises a number of formations, of which Flöttmann et al. (1994) used the thick Heatherdale Shale as the balancing unit. The Heatherdale Shale passes conformably up into the turbiditic sedimentary rocks of the Kanmantoo Group. This unit has been divided into several formations, most recently by Jago et al. (2003). The various formations of the Kanmantoo Group are, from base to top, the Carrickalinga Head Fm, Backstairs Passage Fm, Talisker Fm, Tapanappa Fm Tunkalilla Fm and Balquhidder Fm (Fig. 3).

### 2.2. Regional structure and metamorphism

The arcuate shape of the Delamerian Orogen in South Australia (Fig. 1) has been explained by a combination of the original basin architecture and compression against a curved cratonic margin, involving zones of transcurrent movement (Clarke and Powell, 1989; Belperio and Flint, 1993; Marshak and Flöttmann, 1996).

High temperature, low pressure metamorphism was established early on in both the Delamerian (Dymoke and Sandiford, 1992) and Ross Orogens (Flöttmann et al., 1993b). Metamorphic grade increases eastward, towards the

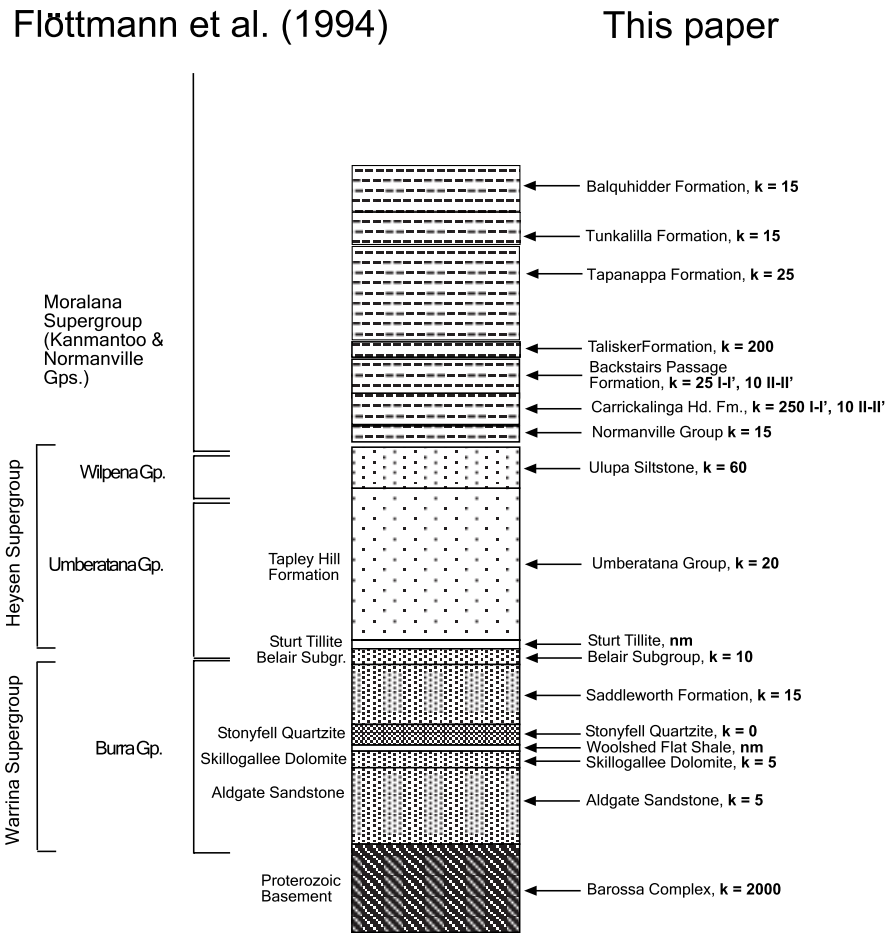


Fig. 3. Simplified stratigraphic column after Flöttmann et al. (1994) showing units chosen as representative for this study. Magnetic susceptibilities used in the replica forward models are also shown in $10^{-5}$ SI units (nm = not modeled). Relative thicknesses are based on those used by Flöttmann et al. (1994) for section balancing, and may not be representative of the strained thicknesses (see Flöttmann and James, 1997).

core of the Delamerian Orogen (Jenkins and Sandiford, 1992), going from chlorite facies in the foreland on the Fleurieu Peninsula, to sillimanite facies and migmatites in the Kanmantoo Group (Fig. 2).

Deformation in the foreland is characterized by inclined to recumbent, asymmetric folds, with shortened overturned limbs that are often cut out completely by west-vergent thrusting directed towards the Late Archean–Proterozoic Gawler Craton (Flöttmann et al., 1994; Yassaghi et al., 2000). The structural architecture of the western core of the Fleurieu Arc is characterized by large-scale macroscopic, upright to inclined, open, similar, N–S-trending, gently S-plunging folds (Figs. 1 and 2) (Mancktelow, 1990; Preiss, 1995a). These rocks are intruded by abundant syn- and post-tectonic granitoids described by Foden et al. (2002). The western part of the belt is cut by steeply dipping reverse faults and high-strain shear zones that have concave to the northwest traces in map view (Flöttmann et al., 1994). Some of these faults, such as the Williamstown–Meadows Fault (Figs. 1 and 2), display strong metamorphic differences between hanging wall and footwall (Dymoke and Sandiford, 1992; Jenkins and Sandiford, 1992) implying many kilometers of dip-slip movement during orogenesis.

Correlatives of the Delamerian Orogen in Antarctica are poorly exposed, but are known to be poly-deformed, due to Neoproterozoic deformations prior to the pervasive Ross Orogeny (Goodge et al., 1991, 1993). In contrast, the Delamerian is the only orogenic event recorded by the equivalent Australian rocks (Preiss, 1995a). Thus, interpretations in Antarctica are complex, as overprinting relationships must be unraveled. Because of this, more highly detailed kinematic models have been proposed for the Delamerian Orogen (Flöttmann et al., 1994), than for the equivalent Antarctic terranes of the Ross Orogen (Flöttmann and Kleinschmidt, 1991).

Flöttmann et al. (1993a,b) correlated the Wilson Terrane in North Victoria Land (Antarctica) with the Delamerian Orogen in South Australia and western Victoria (Australia). They reported broad symmetry of east-over-west displacement at the western orogenic margins, and west-over-east kinematics farther to the east in Victoria and North Victoria Land, respectively (i.e. a doubly divergent 'pop-up' structure). Flöttmann et al. (1993b) noted that the western boundaries were not as good a fit for correlation as structures father east. East-dipping faults in the Fleurieu Arc, which transport material westward towards the Gawler Craton, have been matched with the large-scale Exiles Thrust in North Victoria Land (Flöttmann et al., 1993a,b). However, the clear contact between the Delamerian fold-and-thrust belt and the Gawler Craton is not mirrored by the Exiles Thrust at the edge of the East Antarctic Craton (Flöttmann et al., 1993b). Furthermore, the east–west-trending part of the Fleurieu Arc exposed on Kangaroo Island (Belperio and Flint, 1993) is not seen anywhere in the Antarctic equivalents, which all trend approximately north–south (Flöttmann and Kleinschmidt, 1991). Thus, there are some unresolved problems with using structures in the Ross and Delamerian orogens as piercing points in tectonic reconstructions.

Deformation in the Ross and Delamerian Orogens is characterized by major contractional faults, primarily thrusts and shear zones, as well as regional folding, and has been interpreted to imply up to 58% orogenic shortening (Flöttmann and Kleinschmidt, 1991; Flöttmann et al., 1994). Detailed studies in the Fleurieu Arc (Flöttmann et al., 1994, 1995; Flöttmann and James, 1997; Yassaghi et al., 2000, 2004), have revealed the presence of many thrusts and reverse-slip shear zones, which are modeled in balanced and restorable cross-sections as parts of imbricate stacks (Flöttmann et al., 1994). Involvement of detached basement slices in these models has been invoked on the basis of the outcropping Precambrian basement inliers (Fig. 1). This differs from the style of deformation reported in Antarctica (Flöttmann et al., 1993a,b) where such slivers of detached basement are not recognized. Some relict granulite facies rocks have been identified in isolated nunataks, but their relationship to cover sequences is often ambiguous (Flöttmann and Kleinschmidt, 1991).

Flöttmann et al. (1994) divided the Fleurieu Arc into a series of three structural zones, based on the style of shortening required to balance and restore the deformed cover sequences to their original inferred basinal geometries. Their Zone 1 is a structural foreland (Fig. 5a and b). In the northern section, the foreland comprises flat-lying to shallowly west-dipping cover sequences in an anticline above a ramp-flat system at the basement-cover unconformity. In the southern balanced section, the foreland mostly comprises an overturned syncline of the lower Burra Group, with its eastern limb overthrust by a basement slice (the Normanville Inlier).

Zone 2 of Flöttmann et al. (1994) is an imbricated zone. In the northern balanced section, this zone is bounded by a frontal ramp system in the west and the Williamstown–Meadows Fault to the east (Fig. 5a). Between these two faults, Flöttmann et al. (1994) interpreted five horses of the cover sequence, and two blind, basement-involved thrusts beneath the Onkaparinga (ramp) Anticline. In the southern balanced section (Fig. 5b), the imbricated zone is bounded by the Aaron Creek Fault (east) and the Talisker Fault (west), with four interpreted horses involving both basement and cover.

Zone 3 in the sections is a metamorphic complex, comprising thick, upright folded sequences of the Cambrian Kanmantoo Group with fewer thrusts than in the structural zones to the west (Fig. 5a and b). Flöttmann et al. (1994) and subsequent workers (Yassaghi et al., 2000, 2004; Foden et al., 2002) interpreted this zone (after Mancktelow, 1990) as an inverted, narrow, extensional basin, the Kanmantoo Trough. Flöttmann et al. (1994) interpreted that shortening by folding in this zone was accommodated at depth by a series of

detachments at the level of the Talisker Formation within the Kanmantoo Group. Beneath this weak horizon, shortening was interpreted to be accommodated by imbrication of both the underlying successions of the Moralana, Heysen and Warrina supergroups, and the crystalline basement.

## 3. Methods

### 3.1. Modeling procedure

Both balanced sections (Flöttmann et al., 1994, their fig. 2; transect I–I′ and II–II′, respectively) were scanned at high resolution, rectified, and imported as backdrops into ModelVision Pro v4.00.22 (Encom Technology, 2002), to provide a digitizing template for forward modeling of the magnetic data.

Total magnetic intensity (TMI) data coincident with both sections were extracted from a publicly available South Australian Government dataset (Fig. 4). These data form a composite grid compiled from a variety of surveys, with flight line spacings of between 100 and 400 m, and a drape flying height of 80 m above the ground surface. The final grid cell size is 80 m, meaning that structures or marker units with across-strike length-scales of $<160$ m are not resolvable. The data has been subjected to standard pre-gridding processing and leveling techniques such as those described by Minty et al. (2003). Linear transects (see Fig. 4 for exact coordinates) were extracted from the grid in the program ERMapper v6.0 (Earth Resource Mapping, 2002) and imported as ASCII files into ModelVision Pro.

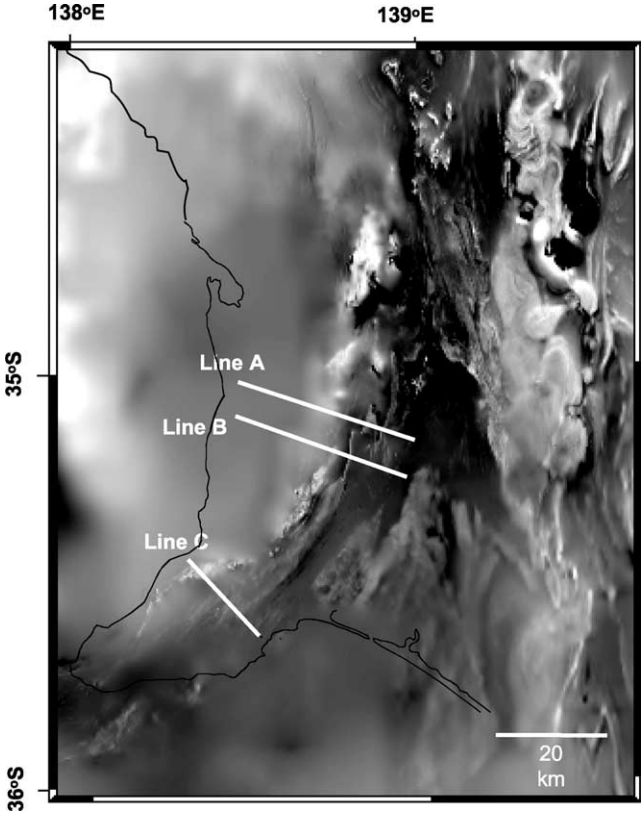


Fig. 4. TMI image extracted from South Australian Government dataset showing the three lines modeled; two of these define a corridor around the Flöttmann et al. (1994) transect I–I′. Note the sharp discontinuous feature between lines A and B, likely to be a parasitic fold. Coordinates of line A are 274756 mE, 6119961 mN to 314954 mE, 6104217 mN; line B is from 272394 mE, 6114939 mN to 312591 mE, 6099195 mN. II–II′ is from 255150 mE 6073200 mN to 275440 mE 6052675 mN. Coordinates are in UTM map zone 54 and are projected into the MGA84 datum.

The process of geophysical forward modeling of cross-section templates has been described by Direen et al. (2001), amongst others. Briefly, it involves assigning rock property data (in this case, bulk average magnetic susceptibilities) to polygons within the template cross-sections. These are then modeled as polyhedra with limited strike extents outside the section plane. The magnetic field response of each polyhedron is computed according to an analytic solution (Lee, 1980), and the results integrated across the section to give a calculated total magnetic field for that section geometry. If a mismatch is observed between the calculated field and the actual observed field along the plane of section, then the interpreter has two choices: either the geometry can be altered, or the bulk properties can be adjusted. The field can then be recalculated. This process is repeated iteratively until the calculated field matches the observed field over the section, to within some acceptable level of fit. Normally the root mean squared (RMS) difference between the modeled and the calculated fields is used as an estimator of goodness of fit, as it reflects the signal to noise characteristics of the observed field data. Further information about this procedure can be found in, for example, Boschetti et al. (1999).

Modeling was undertaken according to the algorithm described in Direen et al. (2001), which describes a procedure for incorporating structural geometric interpretations with constraining geological and rock property data in order to produce admissible geophysical models. Such '2.5D' magnetic forward models were created by digitizing the structure of the Flöttmann et al. (1994) cross-sections, and assigning each polygon a measured bulk apparent susceptibility (Fig. 5).

Forward calculations of the magnetic field were carried out in ModelVision Pro according to the algorithms of Lee (1980) for the analytic solutions of 3D polyhedra. In these calculations, strike extent was limited to 10 km out of the plane of section. Strike lengths given for all bodies were symmetric about the line of section. This was considered reasonable, given the generally simple ca. N–S strike of structures in the Mt Barker area and NE–SW strikes in the southern Fleurieu Peninsula (Figs. 1 and 2). In addition, this assumption reflects those made in the line and area balancing process employed by Flöttmann et al. (1994).

For the I–I′ transect, two magnetic traverses (lines 'A' and 'B'; Figs. 1 and 3) were extracted from the grid, defining a corridor corresponding to the likely limits of structural data projected into the cross-section of Flöttmann

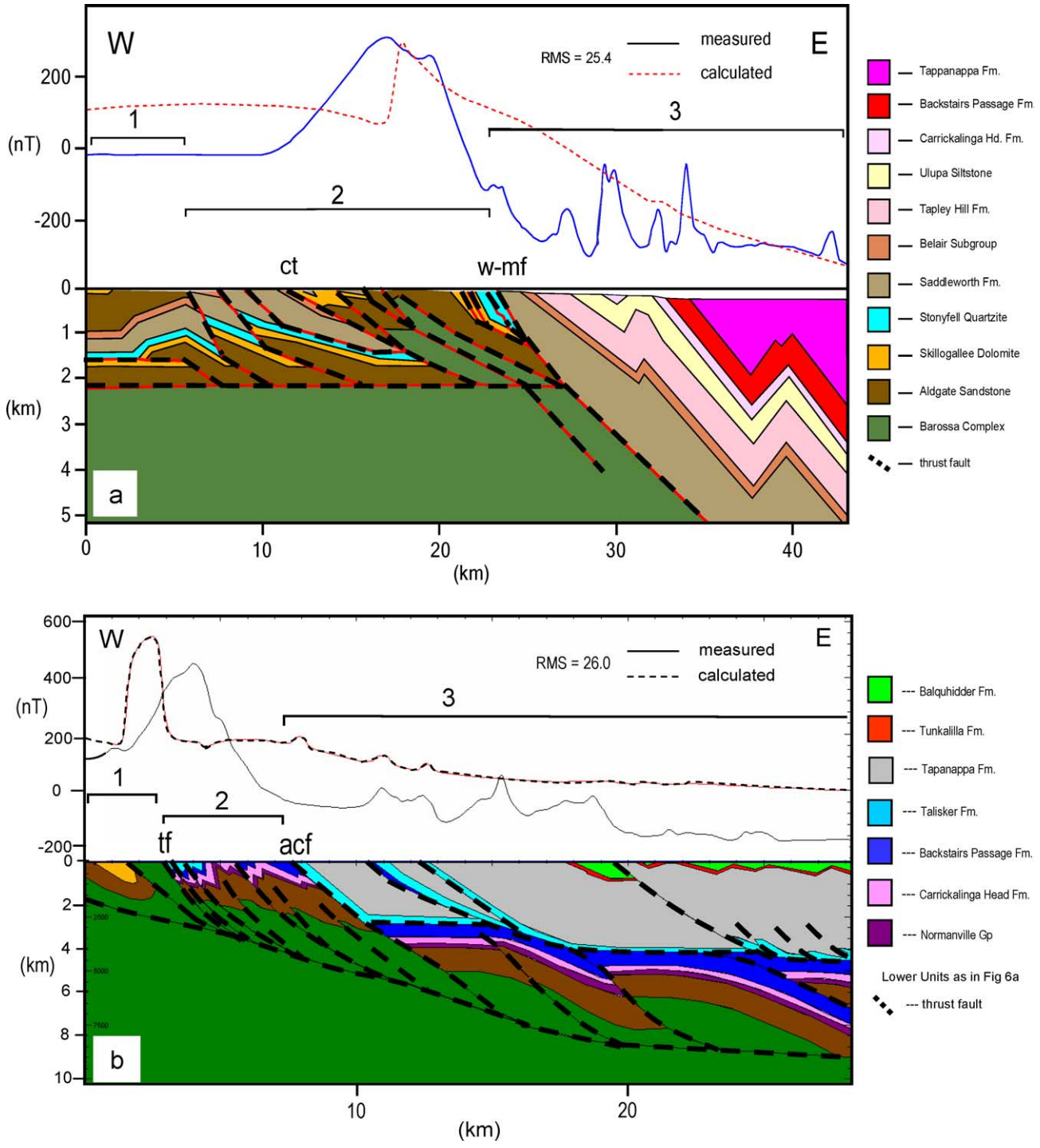


Fig. 5. (a) Replica magnetic forward model for the balanced cross-section I–I′ in Flöttmann et al. (1994, their fig. 2) using data from Table 1 (w–mf = Williamstown–Meadows Fault, ct = Clarendon Thrust; 1–3 refer to the structural zones of different shortening styles classified by Flöttmann et al. (1994, their fig. 3)). (b) Replica magnetic forward model for the balanced cross-section II–II′ in Flöttmann et al. (1994, their fig. 6) using data from Table 1 (tf = Talisker Fault; acf = Aaron Creek Fault; 1–3 refer to the structural zones of different shortening styles classified by Flöttmann et al. (1994, their fig. 6)).

et al. (1994). This procedure also avoids a sharp, discontinuous magnetic feature (likely to be a parasitic fold), which trends obliquely to the strict line of projected section between Green Hills and Macclesfield (Fig. 4). The II–II′ section was modeled on a single line, as there were no out-of-plane complexities that violate the '2.5D' assumptions of the magnetic algorithm used.

Magnetic inversions that predict the distribution of magnetic sources from the observed potential field data (Boschetti et al., 1999) were also conducted on the

cross-sections, testing the sensitivity of combinations of geometry and susceptibility. These inversions were conducted both for individual balancing units, and en masse. The algorithms for inversion in ModelVision Pro are described in Encom Technology (2002).

A regional magnetic field was calculated by ModelVision Pro from the observed data. This was then manually adjusted by adding a positive value to the entire field, to compensate for deep magnetic sources below 5 km depth, which are beyond the depth of the Flöttmann et al. (1994) cross-sections. The positive field shift applied is equivalent to the effect of a thick magnetic slab in the middle crust (Schlinger, 1985), which probably reflects the presence of magnetic basement at depth beneath the Fleurieu Arc.

The estimated regional magnetic field produces some negative residual magnetic anomalies. These may be the result of paramagnetic minerals that carry weak negative magnetic remanence (Clark, 1997). In particular, detrital and metamorphic ilmenite was found in many samples during thin section and microprobe analysis (Brock, 2003, unpublished data). Ilmenite is known to be a significant carrier of minor anomalous negative remanent magnetizations (Clark, 1997). Alternatively, apparent negative susceptibility may be due to early Paleozoic thermoremanent magnetite that has been noted in a few units of the Fleurieu Arc (Klootwijk, 1980; Rajagopalan, 1989).

### 3.2. Sampling procedure for magnetic susceptibility

Bulk apparent magnetic susceptibilities ($k$) were measured using a Geoinstruments JH-8 magnetic susceptibility meter, at numerous locations in the Fleurieu Arc along three main sampling routes (Figs. 1 and 2). These data were cross-checked against an extensive database of susceptibilities for the Kanmantoo Group (Gum, 1998). The combined dataset provides geophysical constraints for the forward models. All measurements were apparent magnetic susceptibilities only, as remanent magnetic effects were not taken into account. As the magnetic field in the local vicinity of a rock is a vector sum of the induced and any 'permanent' remanent field (usually due to a variety of small, localized effects; see Clark, 1997), measured susceptibilities could be damped or amplified by remanence. For simplicity, apparent magnetic susceptibilities are herein referred to plainly as 'susceptibility'.

Susceptibility measurements were obtained for each major stratigraphic unit (Table 1) in the Fleurieu Arc used in the balanced sections of Flöttmann et al. (1994). Three sampling routes were chosen to transect the entire stratigraphic column and to give control on facies-related spatial variation (Figs. 1–3). The main criterion for selection of a sample location was good exposure of a fresh, unoxidised outcrop.

Measurements were taken at regular intervals across strike at outcrops, avoiding highly deformed or fractured rock, mesoscopic geological structures, and obviously weathered zones. At least 30 measurements were taken at each location, with spatial heterogeneity being investigated where possible. This was done by taking measurements on and orthogonal to foliation planes or compositional layering in the rocks. Minor magnetic heterogeneity was observed in some locations, but this was always within the spread of data. More significant variations were observed due to heterogeneity within stratigraphic units, for example between the monotonous pelitic and psammitic beds, and in the Barossa Complex. The significance of this is discussed below.

The major assumption in this study is that observed susceptibility values are representative of the bulk average for each unit at depth , and along strike. Some sample locations are tens of kilometers from the published balanced sections, so the values chosen as constraints were preferentially from the closest sampling route (Fig. 1). The values chosen match well in terms of metamorphic grade, as differences are observed for the same stratigraphic units on the different sampling routes (Fig. 2). Samples from the Gorge Road route (GR: Figs. 1 and 2) were used to provide perspective on the range of acceptable values.

Sampling of the upper Kanmantoo Group (Tapanappa, Tunkalilla and Balquhidder formations) between Tunkalilla and Waitpinga beaches on the south coast (Figs. 1 and 2) indicates very low susceptibilities (average $10–15\times10^{-5}$ SI) for all of these units, a result also confirmed by the dataset of Gum (1998).

No outcrop of the Carrickalinga Head Formation of the Kanmantoo Group was located on the SE sampling route, although some sample localities for this unit are located between routes SE and GR. Most data on this formation thus come from the south coast sampling transect (SC: Figs. 1 and 2). The Carrickalinga Head Formation generally displays low magnetic susceptibilities, similar to the other metasedimentary rocks of the Fleurieu Arc (Table 1). However, Carrickalinga Head Formation outcrops on the GR route are located in the migmatite zone (Fig. 2), and the highest value of $1475\times10^{-5}$ SI was obtained in the immediate vicinity of a significantly magnetic granite intrusion. A value slightly higher than the average of all sample localities was assigned to this formation ($k=250\times10^{-5}$ SI) after the initial iterations of the forward model, to reflect contributions from mafic intrusions that are known to intrude the deepest parts of this succession (Foden et al., 2002).

In the SC sampling transect, several units crop out that are not found in the northern transect, including the Talisker Formation (Flöttmann et al., 1994; also Jago et al., 2003). This stratigraphic unit in the section comprises the Cooalinga Sandstone Member and the Nairne Pyrite Member (Jago et al., 2003). Whereas the sandstone member is relatively non-magnetic ($k=5–30\times10^{-5}$ SI: Gum, 1998), the Nairne Pyrite Member (which contains pyrrhotite) is significantly susceptible (maximum $k=2000$ and $1400\times10^{-5}$ SI, respectively: Gum, 1998).

Table 1
Sample localities and corresponding average apparent magnetic susceptibility ($k$) values with value used in forward modeling (apparent susceptibility measurements are in $10^{-5}$ SI units)

| Stratigraphic unit | SE sample location | SE $k$ value | GR sample location | GR $k$ value | SC sample location | SC $k$ value | $k$ Value used in model |
|---|---|---|---|---|---|---|---|
| *Kanmantoo Group* | | | | | | | |
| Balquhidder Formation | SE 33 | 20 | | | SC1 | 10 | 10 |
| Tunkalilla Formation | | | | | SC5 | 0 | 0 |
| Tapanappa Formation | SE 32 | 25 | | | | | 25 |
| | SE 34 | 20 | | | | | |
| Talisker Formation (value from Gum (1998)) | | | | | | | 200 |
| Backstairs Passage Formation | SE 31 | 15 | GR 19 | 20 | SC 7 | 15 | 25 |
| | | | GR 21 | 40 | | | |
| | | | GR 22 | 30 | | | |
| | | | GR 23 | 20 | | | |
| Carrickalinga Head Formation | GR 11 | 1475 | SC6 | 10 | 250 | | |
| | | | GR 12 | 50 | | | |
| | | | GR 13 | 40 | | | |
| | | | GR 17 | 35 | | | |
| | | | GR 18 | 110 | | | |
| | | | GR 24 | 20 | | | |
| | | | GR 25 | 25 | | | |
| *Normanville Group* | | | | | | | |
| Carbonate value from Gum (1998) | | | | | SC9 | 15 | 15 |
| | | | | | Shales | 11 | |
| | | | | | Carbonate | 240 | |
| *Umberatana Group* | | | | | | | |
| Ulupa Sltstone | SE 18 | 65 | | | | | 60 |
| | SE 29 | 55 | | | | | |
| Tapley Hill Formation | SE 17 | 15 | | | | | 20 |
| | SE 25 | 25 | | | | | |
| Belair Subgroup | SE 26 | 15 | | | | | 10 |
| | SE 28 | 0 | | | | | |
| Saddleworth Formation | SE 8 | 20 | | | | | 15 |
| | SE 24 | 10 | | | | | |
| Stonyfell Quartzite | SE 6 | 10 | GR 2 | 5 | | | 0 |
| | SE 7 | 0 | GR 3 | 0 | | | |
| | SE 24 | 0 | | | | | |
| Skillogallee Dolomite | | | GR 6 | 5 | | | 5 |
| | | | GR 7 | 5 | | | |
| Aldgate Sandstone | SE 9 | 5 | | | | | 5 |
| | SE 11 | 10 | | | | | |
| | SE 22 | 0 | | | | | |
| | SE 23 | 0 | | | | | |
| *Palaeo- to Mesoproterozoic basement* | | | | | | | |
| Barossa Complex | SE 12 | 25 | GR 8 | 1575 | SC8 | 30 | 2000 |
| | SE 15 | 20 | GR 8a | 4060 | | | |
| | SE 20 | 40 | GR 8b | 4000 | | | |
| | SE 21 | 580 | | | | | |

Other parts of the Kanmantoo Group in the SC transect, such as the Carrickalinga Head Formation ($k$ mean $= 10 \times 10^{-5}$ SI) and Backstairs Passage Formation ($k$ mean $= 10 \times 10^{-5}$ SI) have been assigned lower bulk magnetic properties from those in the north, on the basis of field observations. The lower bulk susceptibility of the Kanmantoo Group on the south coast may reflect lower metamorphic magnetite content, as these rocks are farther removed from the high grade sillimanite and migmatite zones of the orogen (Fig. 2) and have no recognized mafic intrusions.

The only constraining data acquired for the Normanville Group were from the Heatherdale Shale (Fig. 3). Other formations within this group, principally carbonates, were not measured in this study. Rajagopalan (1989) measured very low ($k = 0$–$50 \times 10^{-5}$ SI) susceptibilities throughout the Normanville Group, consistent with our assumption that the magnetic properties of the Heatherdale Shale are representative of the whole group. The value assigned is also consistent with the approach of Flöttmann et al. (1994), who did not include separate subdivisions of the Normanville Group in their balanced sections.

Measurements from the rocks of the Adelaide Rift

Complex—the Heysen and Warrina supergroups—are also summarized in Table 1 and Fig. 3. All formations measured, with one exception, recorded low or zero magnetic susceptibilities, only ranging up to $25\times10^{-5}$ SI units in some of the shales. The purer quartzites/sandstones and dolomites all recorded values close to zero. The highest average value recorded was from the Ulupa Siltstone of the Wilpena Group, which was accorded a moderately low value of $60\times10^{-5}$ SI units.

The Barossa Complex displays a wide range of measured susceptibilities, including the highest measured values in this study, over $4000\times10^{-5}$ SI units (Table 1). Data from all sampling routes were considered equally when assigning a bulk average magnetic susceptibility value for the Barossa Complex, as the multiple populations of susceptibilities are interpreted to reflect localized lithological interlayering (Rajagopalan, 1989; Paul, 1998) rather than a spatial dependency across the orogen. The high susceptibility eventually assigned to the Barossa Complex ($k=2000\times10^{-5}$ SI) is interpreted to be representative of its bulk magnetic properties at depth.

## 4. Results

### 4.1. Potential field data

Before modeling the magnetic field, it is necessary to appraise its characteristics, as the amplitude and spatial frequency of magnetic anomalies can provide qualitative information about the 3D geometries of the associated rocks (Leaman, 1997).

The magnetic field in the plane of section I–I′ (lines A and B; Fig. 4) is flat and slightly negative (−15 nT) for the first 10 km of section (Fig. 4) over the area associated with the Adelaide plains. The field then rises smoothly to its highest value (+310 nT) at a point 18 km along the section. The half wavelength of this anomaly is ca. 12 km, and has a superimposed double peak of 260 nT at ca. 20 km. The field falls off sharply to a value of ca. −260 nT by 26 km along the section. Farther to the SW, the field maintains a base level of ca. −250 nT, but with a series of superimposed peaks of ca. 2 km wavelength, ranging in amplitude between 90 and 260 nT, peak to peak. In the magnetic imagery (Fig. 4), these peaks are associated with the trace of a macroscopically folded magnetized sedimentary horizon. Off the eastern end of the section is a low magnetic region, showing further macroscopic folding, which then passes into a zone of ellipsoidal magnetic highs associated with the granites that intrude the higher (migmatite) grade core of the fold belt.

The magnetic field in section II–II′ (Line C; Fig. 4) is higher at its northeastern end, at around +110 nT. It rises steeply to a value of +450 nT at 4.5 km, forming an anomaly with half wavelength of ca. 6 km. The field then decreases steeply to a value of −60 nT at a distance of 9 km, and then decreases much more gradually to a value of −160 nT at the end of the profile. Superimposed on this shallow, negative magnetic field gradient are a series of lower amplitude anomalies, of between 20 and 160 nT peak to peak amplitude, and half wavelengths of around 1–2 km. In the magnetic image, the anomalies between 10 and 20 km distance are associated with the trace of a macroscopic folded horizon. Beyond 20 km, the magnetic field is bland, with very low amplitude responses.

### 4.2. Modeling results

There is a poor match between the observed and calculated magnetic responses if the geometry of the Flöttmann et al. (1994) balanced cross-sections are used in the forward models (Fig. 5a and b). This suggests the models are invalid according to the conditions of De Paor (1988).

#### 4.2.1. Section I–I′

In the western half of this transect, the forward model geometry requires a high amplitude, high frequency magnetic response with a single sharp asymmetric peak, compared with the long wavelength, high amplitude, more symmetric observed magnetic response (Fig. 5a). The metasedimentary rocks in this sector are of the Warrina and Heysen supergroups, and all units showed low magnetic susceptibilities in outcrop (Table 1). The corresponding modeled magnetic signature is characterized by a smooth, low frequency response, as expected from these properties. The observed lack of magnetic contrast between the various strata within the metasedimentary cover sequences in structural zones 1 and 2 makes it difficult to comment on the validity of the complex imbricate thrusting proposed in the Flöttmann et al. (1994) model; however, the prediction of discrete thrust-bounded wedges of magnetic basement predicted by this model clearly cannot fit the TMI data.

The initial model based on the balanced section also fails to calculate a sufficient response in the eastern half of the transect, where the Kanmantoo Group (Fig. 5a) is exposed immediately southeast of the Macclesfield Syncline. The magnetic field here displays many high frequency anomalies compared with zones 1 and 2, demanding more significantly magnetized horizons than are observed in the outcrops on the sampling routes.

Further experimental forward modeling (not shown) of the deformed Kanmantoo Group indicates that susceptibility values of between 2000 and $6000\times10^{-5}$ SI units are required to match the amplitudes of the anomalies, giving a subsequent RMS fit of 7. These susceptibility values are well in excess of the maxima for these pelitic and psammitic rocks observed in outcrop (see Fig. 4 and Table 1). Moreover, these high values are restricted to horizons much thinner than the formations used by Flöttmann et al. (1994) to balance their section around the Macclesfield

Syncline, and do not appear to be continuous at depth, as they cannot be modeled continuing around the fold hinge.

This problematic distribution of magnetized sources within the Kanmantoo Group may be, in part, due to magnetic inhomogeneity, corresponding to intercalation of distinct pelitic and psammitic lenses (Rajagopalan, 1989; Jago et al., 2003). However, the observed magnetic contrast between these bulk compositions is still small (Table 1); it is much more likely that the anomalies are caused by sulfide-mineralized horizons within the Talisker Formation that contain significant amounts (up to 6%) of magnetized pyrrhotite, and which are known to be discontinuous at depth (Belperio et al., 1998). Gum (1998) recorded values of up to $2000\times10^{-5}$ SI for thin, sulfide-mineralized pods within the Talisker Formation, agreeing well with our interpretation of the experimental forward modeling.

The overall style of upright, fold-dominated shortening and lack of observed basement involvement in the deformation of the Kanmantoo Group in structural zone 3 (Flöttmann et al., 1994) is in agreement with the extensive outcrop control in the Macclesfield Syncline (Sprigg and Wilson, 1954); consequently, because of the dominance of the magnetic signal by the magnetized, discontinuous horizons described above, which also suggest upright folding of the Kanmantoo Group, we have concluded that this part of the section is geophysically admissible, and have chosen not to further test it.

### 4.3. Inversion results

Inversion of the Flöttmann et al. (1994) cross-section over line A, whereby only rock properties were allowed to vary (i.e. the geometry remained unaltered) improved the RMS fit of the data to 5.1 (Fig. 6). However, the inverted forward model is also unacceptable for two main reasons.

First, although the RMS fit is improved, there is still a poor match between the calculated magnetic signature and the observed signal (Fig. 6). The low frequency, high amplitude observed signal in the western part of the transect is poorly matched by the high frequency modeled signature from near surface, high susceptibility rocks required by the inversion. The eastern part of line A has the opposite situation, where the calculated signal is characterized by low frequency, compared with the higher frequency signal of the observed TMI data. This is primarily due to the distribution of mineralized members discussed above.

The second, and more important, reason for the inadmissibility of the inverted model is the disparity between the observed bulk magnetic susceptibilities of rocks in the field and bulk values assigned to those units in the inversion process. Measured susceptibilities were relatively uniform for most stratigraphic units except the magnetically high Barossa Complex and Carrickalinga Head Formation (Fig. 3; Table 1). Inversion of the geometric model produces unreasonable bulk magnetic susceptibility values compared with the ranges of the measured rock property constraints. Susceptibility values required by the inversion process are up to two orders of magnitude too high for most of the units in the balanced section, which is unacceptable when compared with the field measurements (Table 1).

The lack of any significantly magnetic Neoproterozoic sedimentary rocks identified in this study suggests the basement alone is the simplest explanation for the large amplitude magnetic signal in the western half of the transect, despite the multiple populations of susceptibilities within that unit (Table 1).

Inversion of the data with a fixed high magnetic susceptibility value for the Barossa Complex shows that the model is highly sensitive to the geometry of the basement, highlighting its importance for the outcome of the forward model. The inversion process can therefore be used to give an unbiased estimation of the spatial distribution of magnetic basement in the subsurface, thus placing an independent constraint on the balanced section geometry where blind basement involvement has been inferred.

Further magnetic forward and inverse modeling was undertaken to elucidate possible magnetic sources and their geometries, especially where the structural model predictions were in serious disagreement with the observed fields. Detailed geometric models incorporating these findings for both the western and eastern halves of balanced section I–I′ are difficult to construct without more comprehensive and detailed measurements of susceptibility, and further geological constraints. However, some basic geometrical arrangements for the distribution of magnetic Barossa Complex were modeled to try to match the magnetic and susceptibility data, in order to provide constraints on future balanced cross-section construction. These models are speculative, due to a lack of dip constraints at depth, a lack of information on the representativeness of the different magnetic populations within the Barossa Complex, and the inherent non-uniqueness of forward models (Boschetti et al., 1999).

The simplest geometry matching the data is a large region of elevated basement (Figs. 7–9) rather than imbricate, discrete wedges bounded by shallow east-dipping thrusts. This structure can be interpreted in a number of ways, each of which has different bulk shortening ramifications. The first possibility is that this structure is a simple, upright anticline, representing basement shortening by folding beneath structural zone 2 of the Flöttmann et al. (1994) section.

The next possibility tested was a ramp anticline structure for line A. This could be either a ramp anticline above a blind basement thrust, or an antiformal stacked duplex (Fig. 7). The magnetic signal is insensitive to the number of sheets that could form the latter structure. If this alternative geometry is correct, and assumptions about the bulk distribution of susceptibility within the basement are valid, the crest of this structure would lie at relatively shallow depths (minimum 780 m; Fig. 7). This model is

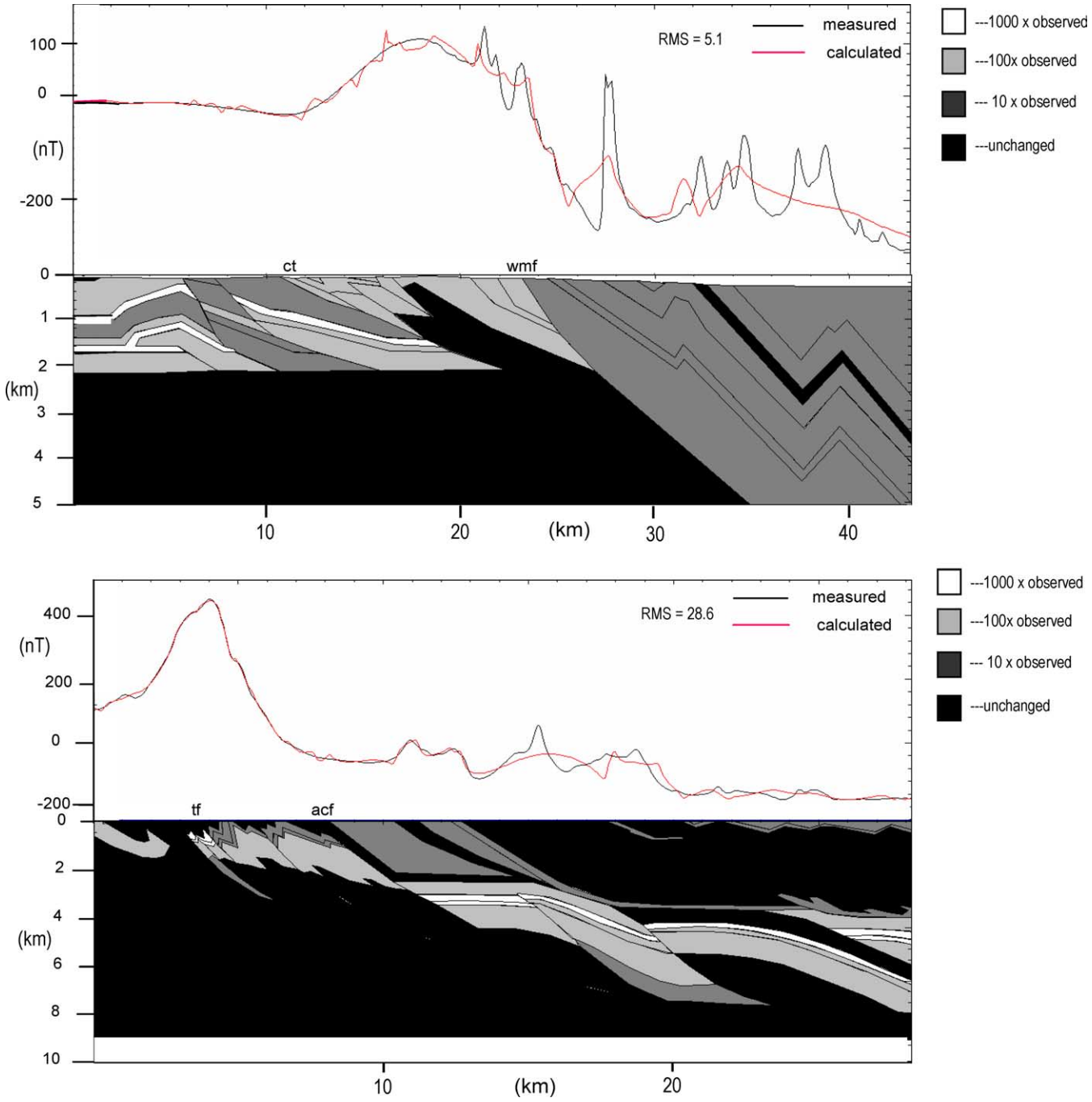


Fig. 6. (a) Inverted, replica forward model for the Flöttmann et al. (1994) cross-section over line A. (b) Inverted, replica forward model for the Flöttmann et al. (1994) cross-section over line C. In both models, note the high susceptibilities assigned to units that are clearly non-magnetic according to field observations.

consistent with observations of basement outcrops both north and south of line A as anticlinal cores (Fig. 1), which have faulted western and unconformable eastern margins (Preiss, 2003).

This model may be tested by further investigations of the overall dip of the fold enveloping surface in structural zones 1 and 2. According to our simple model, the enveloping surface in both zones should both dip to the west; this is opposite to the prediction of the Flöttmann et al. (1994) section, which shows westerly or flat dips in the foreland (zone 1), and a series of slices with east-dipping enveloping surfaces in zone 2.

The high frequency magnetic anomalies on the eastern side of the low frequency, high amplitude magnetic high in line B were modeled by a number of thin, very near-surface slices of basement on the eastern edge of the elevated basement (Fig. 8a). This is somewhat similar to the basement slice geometry of Flöttmann et al. (1994), and also reminiscent of the complex structure described by Preiss (1997) several kilometers north of this transect.

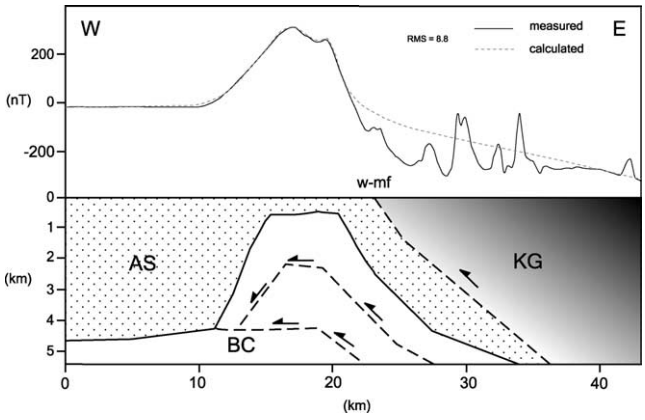


Fig. 7. Ramp-anticline or stacked duplex model, for the western sector over line A. Solid lines represent sedimentary or unconformable contacts and dashed lines, fault contacts (w–mf = Williamstown–Meadows Fault, AS = Adelaidean, KG = Kanmantoo Group, BC = Barossa Complex).

Overall, the cross-section of Preiss (1997) disagrees with the large antiform modeled in our study; however, his mapping of both east- and west-dipping stratigraphy does lend some support to the models for line B.

A steeper dip than interpreted by Flöttmann et al. (1994) for the major Williamstown–Meadows Fault provides a better match to the observed magnetic signal (Fig. 8b). The thin slices of basement in the models for line B could be explained by late brittle deformation at this fault zone, where some post-metamorphic movement is implied by the juxtaposition of different metamorphic grades (Jenkins and Sandiford, 1992; Preiss, 1995a,b).

These small, near surface slices of basement could also have be detached basement horses from early thrusting (Flöttmann et al., 1994; Marshak and Flöttmann, 1996) at the competency boundary between the basement and the overlying cover sequences during the Delamerian Orogeny (Paul, 1998).

A further alternative is that these may be slivers displaced by out-of-plane transpression on the Williamstown–Meadows Fault. This latter alternative is consistent with reactivation of the Williamstown–Meadows Fault as a positive half-flower structure, as occurs in transpressional orogenic systems (Goscombe et al., 2003).

A deep west-dipping geometry for the Williamstown–Meadows Fault gives an even better fit for the eastern side of the major magnetic anomaly (Fig. 9). Such a structure could conceivably represent a buried east-vergent backthrust of basement, forming a triangle zone (Fig. 9a). Such a model would have quite different ramifications for the overall kinematic history of the Fleurieu Arc, and is quite different to the shallow east-dipping listric faults predicted by Flöttmann et al. (1994). However, there is no field evidence described for such an early set of west-dipping thrusts. If this model were correct, then the projection of the east-directed thrusts should emerge in the present hanging wall of the Williamstown–Meadows Fault. No such thrust has been mapped, so it is unlikely that this kinematic alternative is correct, despite the better geophysical fit.

If the steep westerly dip of the Williamstown–Meadows Fault is correct, this zone may be better interpreted as a non-magnetic lithological unit of the Barossa Complex, or a Delamerian intrusive body, neither of which are necessarily thrust bound (Fig. 9b). Both of these alternatives are admissible upon consideration of the regional geological constraints.

#### 4.3.1. Section II–II′

The westernmost domain in the model is the structural foreland, consisting of an asymmetric syncline of Adelaidean metasedimentary rocks with an overturned eastern limb. This westernmost domain corresponds to a magnetically low amplitude, long wavelength anomaly some 1.5 km wide, consistent with the observed low magnetic susceptibilities of the Adelaidean units to the north.

Between 1.5 and 7.5 km along the transect, between the Talisker and Aaron Creek Faults (Fig. 5b), the interpreted imbricate zone of Kanmantoo Group metasedimentary rocks coincides with an observed long wavelength, high amplitude magnetic signal.

The forward model of the balanced section that requires high spatial frequency repetitions of magnetic and non-magnetic units produces a very poor fit of the calculated magnetic response to the observed field, with an RMS fit of 26.0. The response in the imbricate zone is dominated by the magnetic Barossa Complex basement, which crops out near the western end of the section as a phyllonitic fault slice. In the modeled section, the magnetic high produced by this slice is of approximately the right amplitude, but is westward shifted from the magnetic high in the observed field. This result suggests that the bulk of the magnetic basement slice must reside at shallow depths under the imbricated zone interpreted by Flöttmann et al. (1994).

The third structural domain interpreted by Flöttmann et al. (1994) lies to the east of the Aaron Creek Fault (Fig. 5b), and is characterized by folding and buckling above a sub-horizontal detachment at between 2.5 and 4 km depth in the balanced section. The bulk of the folding occurs in the turbiditic units of the upper Kanmantoo Group (Tapanappa, Tunkalilla and Balquhidder formations). This structural domain coincides with a generally negative magnetic signal, punctuated by low amplitude, medium spatial frequency ($\sim$2–4 km wavelength) responses. In this area, the overall pattern of magnetic responses is not reproduced by the structural model—the calculated field is 150 nT too high, and too ‘flat’. The failure to model the significant features in the magnetics is most likely due to two potential errors in the balanced section: the assumption of a sub-horizontal detachment, and the blind magnetic basement surface beneath the Kanmantoo Group being too elevated with respect to the topographic surface.

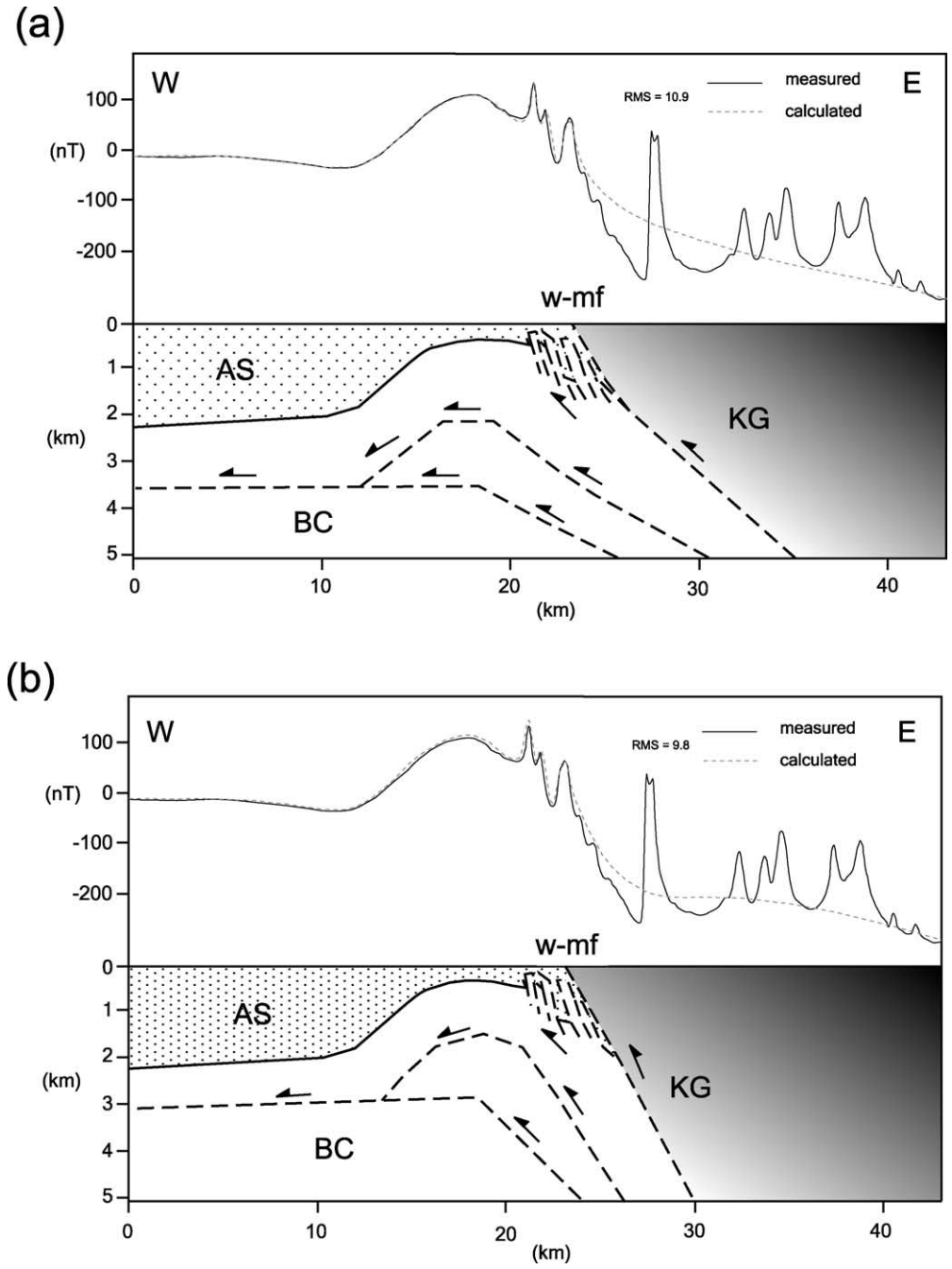


Fig. 8. (a) Ramp-anticline or stacked duplex model, with slices of basement removed from the eastern limb of the antiform. (b) Steeper dip for the eastern limb of the antiform. Line B—solid lines represent sedimentary or unconformable contacts and dashed lines, fault contacts (w–mf = Williamstown–Meadows Fault, AS = Adelaidean, KG = Kanmantoo Group, BC = Barossa Complex).

### *4.4. Inversion results*

An inversion in which only the magnetic susceptibility was allowed to vary resulted in an improvement of the RMS fit of the data ~1000% to 2.8 (Fig. 6b). Although this model has a much better fit, this has been achieved by unrealistic alterations to the susceptibility ranges of many units.

In some cases, particularly in the folded eastern domain, the fit is achieved by making units at depths of >2.5 km, nominally in the lower Moralana Supergroup (Talisker Formation and Normanville Group), significantly negative. This could imply some significant component of negative remanence in the deeper parts of the inverted Kanmantoo Trough. Alternatively, it can be interpreted that these units are offsetting the effect of the magnetized basement being too regionally elevated in the balanced section geometry. Similarly, parts of the Adelaidean metasedimentary rocks deep in the section

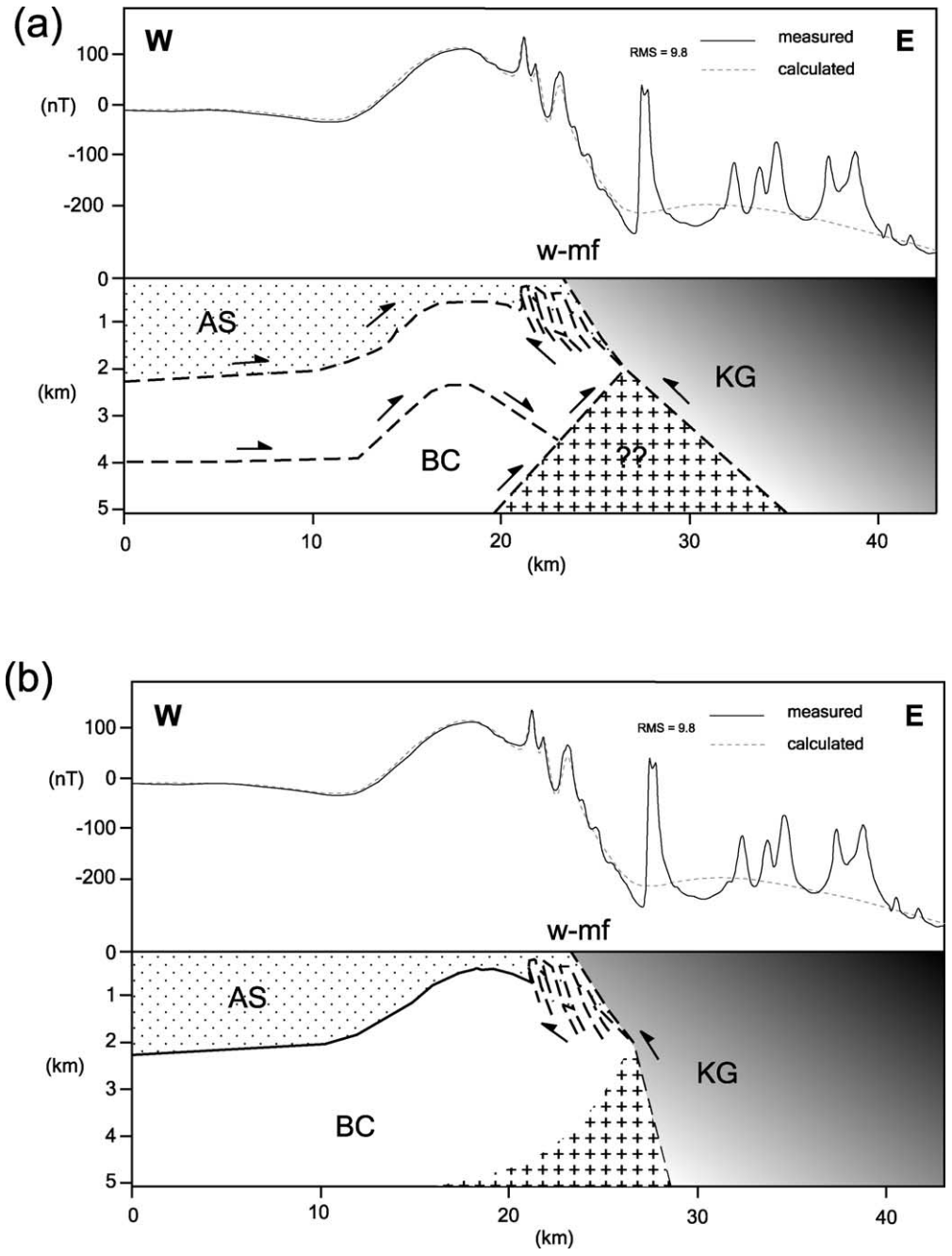


Fig. 9. (a) Fault bounded, non-magnetic triangle-zone formed at merging hinterland-vergent thrust and Williamstown–Meadows Fault. (b) Non-faulted, non-magnetic zone beneath west dipping, magnetic material. Line B—solid lines represent sedimentary or unconformable contacts and dashed lines, fault contacts (w–mf = Williamstown–Meadows Fault, AS = Adelaidean, KG = Kanmantoo Group, BC = Barossa Complex).

are also given unlikely high negative susceptibilities. This suggests that the inverted distribution of rock properties is an artifact, caused by unnecessary elevation of basement during balancing and restoration. Regardless of which interpretation is correct, both alternatives suggest that the cover sequences east of the Aaron Creek Fault are significantly thicker than assumed by Flöttmann et al. (1994). This result is in accord with the findings of Foden et al. (2002), who suggested the genesis of granites from the lower Moralana Supergroup in positions at or near the base of the crust, obviously requiring significant depositional thicknesses of these rocks.

In the imbricated zone, major improvement is achieved by shifting the locus of high susceptibility out of the western basement slice, and increasing the susceptibility of basement units in the immediate hanging wall of the Talisker Fault. This result is consistent with the significant variability of susceptibility encountered within the Barossa Complex. However, the extension of high susceptibility values to

around 1 km shallower than predicted by the structural model (500 m versus 1.5 km) may mean basement in this zone extends to higher crustal levels than previously thought, and that the Normanville Group and lowermost Kanmantoo Group are not present in the frontal horses of the imbricated zone, at least in the plane of the section. Elsewhere, to the south of the section, the Normanville and Kanmantoo groups are present in outcrop exposures. Thus, their absence in the plane of the modeled section is likely due to tectonic excision.

An alternative possibility is that magnetization in this zone may be related to the intense shearing associated with the leading edge of the thrust stack. However, measurements of the magnetic susceptibilities of quartz–muscovite phyllonites in shear zones in the footwall of the Talisker Fault indicate very low to zero values for these rocks, tending to mitigate against this alternative.

## 5. Discussion

The strong magnetic property contrasts measured between the basement and cover sequences in the Fleurieu Arc of the Delamerian Orogen mean that magnetic modeling and inversion can be used to provide geometric constraints on the gross disposition of rock packages in this orogen. The presence of significantly magnetized rock units that correspond to structural marker and balancing horizons within the cover sequences allows testing of the viability of some proposed shortening mechanisms because repetition of these units by folding, thrusting or thickening within a foreland fold-and-thrust belt can produce distinctive and diagnostic magnetic signatures.

However, we caution that where the structure is spatially complex over length scales less than that of the magnetic data ($<160$ m), the method lacks diagnostic resolution. The methods are also not generally transferable to other orogenic systems without a good understanding of rock property distributions in basement and cover sequences (i.e. is there a useful, significant contrast within the orogenic system), the causes of magnetization (e.g. primary lithological versus metasomatic magnetite), and an existing model of how the deformation has redistributed the magnetized markers (e.g. transposition or polydeformation fabrics would tend to defeat the method).

In the southern Fleurieu Arc of the Delamerian Orogen, Flöttmann et al. (1994) suggested three structural zones were defined by their balanced cross-sections (indicated on Fig. 5): (1) a west-dipping to flat-lying foreland; (2) an imbricate zone of faulting; and (3) a metamorphic complex.

The first structural zone was interpreted to consist of a mildly deformed anticlinal structure, possibly a ramp anticline, formed from a frontal ramp at the base of a master detachment above the crystalline basement. The magnetic modeling indicates that this style of fold-dominated deformation may be present beneath both zones 1 and 2, with the basement being fully involved rather than detached (Fig. 7).

The second zone interpreted by Flöttmann et al. (1994) (zone 2, Fig. 5a) requires significant shortening of both basement and cover sequences, accommodated by imbricate thrusting and folding. However, our magnetic models indicate that the disposition of basement slices within the second structural zone of the Fleurieu Arc is not consistent with the geometry required by Flöttmann et al. (1994) to balance their sections. Instead, the simplest explanation of the basement geometry consistent with the magnetic field data implies that the basement forms a large folded structure, which may or may not be cored by thrusts. Outcrop patterns on geological maps (Sprigg and Wilson, 1954; Preiss, 2003) support a simple anticline interpretation for the elevated basement, which requires much less basement shortening than the imbricate model of Flöttmann et al. (1994). An anticlinal basement core agrees with the original interpretation of more fold-dominated deformation in the Fleurieu Arc, where shear zones and thrusts were only considered a minor aspect of the deformation style (Sprigg, 1946; Offler and Fleming, 1968; Mancktelow, 1990).

Alternatively, the structure beneath the imbricated zone may be quite complex, for example, thrust-transected sheets, as suggested by Preiss (1997). Such a structure involving offsets of the cover as well as the basement cores at relatively small length scales may not be able to be fully resolved and modeled with the existing airborne geophysical data. However, such small-scale complexities could be tested by modeling ground magnetic data with a frequency content appropriate to the scale of structures to be resolved.

Flöttmann et al. (1994) suggested that lower levels of the imbricate zone (zone 2, Fig. 5b) were exposed in the east of the Fleurieu Arc by the current erosional surface, where observed faults dips are shallower. This shallowing of dips could be indicative of a fanning pattern of faulting against a basement buttress. Morley (1988) suggested that a ‘sticking point’ at a competency boundary, such as a buttress, is one of the main causes of out-of-sequence thrusting. Flöttmann and James (1997) interpreted deeply incised normal faults throughout the Kanmantoo Trough as forming footwall buttresses along which strain was partitioned, involving basement during the Delamerian Orogeny. This provides some support to the interpretation of the Williamstown–Meadows Fault, interpreted by Flöttmann and James (1997) as the primary growth fault of the Kanmantoo Trough, with the footwall basement block as shown in Figs. 8 and 9. The systematic variation in dips that Flöttmann et al. (1994) interpreted as the eastward shallowing of an imbricate fan to the east may instead be indicative of the opposite situation, in the sense that large, shallow magnetic basement blocks in the west may have forced thrusting at steeper dips as deformation ramped over a sticking point of elevated basement, e.g. the footwalls of the Williamstown–Meadows and Aaron Creek Faults. This is supported by our interpretation that the non-magnetic Adelaidean strata are

very thin in section I–I′, and the large amount of shortening calculated by Flöttmann et al. (1994) (~55%) and Preiss (1997) (~65%), may be the result of competency differences between the thin, laminated cover of the basin feather edge, and a stronger, thicker, heterogeneous basement. In general, magnetic forward modeling confirms the assertion of Flöttmann et al. (1994) that the Williamstown–Meadows Fault marks a large increase in the depth to crystalline basement, thus marking a basement 'buttress'.

The modification of the deep geometry of this buttress by later inversion can be well constrained by the magnetic modeling, as there is a strong magnetic contrast across it. The modeling suggests that the fault is much steeper than predicted by the balanced sections of Flöttmann et al. (1994); we interpret this, together with the presence of detached basement slivers within the fault zone, as the first evidence for transpressive convergence in this part of the Fleurieu Arc.

Flöttmann et al. (1994) interpreted the Clarendon Thrust as the principal décollement above which basement is involved in thrusting (Fig. 5). The implication that further non-magnetic Adelaidean packages exist below a deep-biting Clarendon Thrust is not supported by the magnetic modeling (compare Figs. 5 and 7). Thus, the Clarendon Thrust may represent only a minor accommodating splay from the roof thrust of a major, folded cover-basement detachment. Such a scenario is geometrically and kinematically similar to that originally postulated by Jenkins (1990, see his fig. 7).

The reinterpretation of the deeper parts of the Fleurieu Arc consistent with the magnetic modeling and inversion necessitates a re-evaluation of the shortening mechanisms associated with the formation of the Flerieu Arc. This is not attempted in this paper. However, because of the correlation of the Fleurieu Arc with the northern portion of the Ross Orogen in northern Victoria Land (Flöttmann and Kleinschmidt, 1991), any such re-evaluation will also have implications for the understanding of the broader tectonic system.

Shortening mechanisms in the Ross Orogen in northern Victoria Land (Flöttmann and Kleinschmidt, 1991) and the central Transantarctic Mountains (Goodge et al., 1991) are characterized by large-scale, moderately dipping (40°) to high angle ductile shear zones with dominantly orthogonal reverse movements. However, in places, shallowly plunging mineral elongation lineation fabrics in the thrust planes (e.g. 20° in the Exiles Thrust; Flöttmann and Kleinschmidt, 1991) or shear zone parallel lineations (Goodge et al., 1991) can be used to infer transpressional, oblique shortening in northern Victoria Land. Because of the lack of exposures of the thrust systems, kinematic reconstruction of the amount of shortening accommodated by thrusting versus folding, and amount of orogen-parallel translation is unable to be estimated.

It is clear that the overall shortening style in the Fleurieu Arc, as indicated by our magnetic modeling, with shortening being achieved by a combination of a few large ductile thrusts involving basement and folding of both basement and cover during transpressive reactivation of early-formed basin structures, is consistent with the observations in the Ross Orogen. Moreover, the general pattern of transport directions, as shown by Flöttmann and Kleinschmidt (1991) for various localities in the Fleurieu Arc and the Exiles Thrust system in northern Victoria Land, which have both steep and shallowly plunging lineations through a 90° arc, are consistent with a degree of transpressional convergence in the wider Ross–Delamerian orogenic system.

## 6. Conclusions

We have shown an example of the systematic geophysical testing of balanced cross-sections in a fold–thrust belt that lacks depth constraints imposed by seismic reflection data. Our example, from the Fleurieu Arc of the early Paleozoic Delamerian Orogen in South Australia has a relatively well-modeled strain and kinematic history based on intensive study of structures in outcrop. Attempts have been made to reconstruct the tectonic history of this part of the wider Ross–Delamerian Orogen using balanced and restorable cross-sections. The strong bimodality of magnetic susceptibility between the basement and cover sequences and the presence of significant magnetic marker horizons can be combined with these structural models predicting how the magnetized units have been redistributed in the subsurface. The spatial distribution of these units produces distinctive magnetic anomalies that can be measured from aircraft.

Forward modeling and inversion of airborne magnetic data, using the balanced cross-sections of Flöttmann et al. (1994) across the Fleurieu Arc as constraints, shows significant discrepancies between structural models for the Delamerian Orogen and what is permitted by the observed geophysical and rock property data. Due to its strong magnetic contrast, it can be shown that larger volumes of magnetic basement are present at shallower depths, especially beneath the frontal imbricate zone of the orogen, and that the distribution of basement blocks is unlikely to be in the form of thin, east-dipping slices. Our results indicate that a simpler fold–thrust dominated structural architecture, rather than the imbricate fan models of Flöttmann et al. (1994), may be more appropriate for determining the kinematics in this part of the orogen.

Disposition of basement blocks is still consistent with the presence of west-directed reactivation of original down-to-the-east extensional basement faults, as suggested by Flöttmann et al. (1994), but where basement shortening is more likely accommodated by folding and thrusting, rather than imbrication. The steepness of some of these original structures, and their association with basement-cored anticlines resembling positive half-flower structures (Goscombe et al., 2003), is suggestive of transpressional

orogenesis, rather than a simple orthogonal translation of cover sequences over the Proterozoic basement.

This study has implications for Ross Orogen in Antarctica, where detailed structural and kinematic models cannot be constructed because of lack of suitable exposures. Our results indicate that the simpler fold–thrust dominated architecture described by Flöttmann and others in northern Victoria Land (Flöttmann and Kleinschmidt, 1991; Flöttmann et al., 1993a,b) may be more typical of all Ross–Delamerian shortening. A transpressional shortening model for the Ross–Delamerian orogenic system, as postulated here, is consistent with the overall accretionary plate margin setting interpreted for this orogen (Direen and Crawford, 2003).

## Acknowledgements

We thank Peter Betts, Wolfgang Preiss and Chris Clark for reviews that significantly improved this manuscript, and Andy Burtt (Geological Survey Branch, Primary Industries and Resources, South Australia—PIRSA) for discussions that assisted this research. Justin Gum (PIRSA) is also thanked for alerting us to his magnetic susceptibility database of the Kanmantoo Group. This research was funded by an ARC SPIRT Grant with PIRSA.

## References

Ameglio, L., Vigneresse, J.L., 1999. Geophysical imaging of the shape of granitic intrusions at depth: a review. Geological Society of London, Special Publications 168, 39–54.

Belperio, A.P., Flint, R.B., 1993. Geological note: the southeastern margin of the Gawler Craton. Australian Journal of Earth Sciences 40, 423–426.

Belperio, A.P., Preiss, W.V., Fairclough, M.C., Gatehouse, C.G., Gum, J., Hough, J., Burtt, A., 1998. Tectonic and metallogenic framework of the Cambrian Stansbury Basin–Kanmantoo Trough, South Australia. AGSO Journal of Geology and Geophysics 17 (3), 183–200.

Betts, P.G., Valenta, R.K., Finlay, J., 2003. Evolution of the Mount Woods Inlier, northern Gawler Craton, Southern Australia: an integrated structural and aeromagnetic analysis. Tectonophysics 366, 83–111.

Black, L.P., Sheraton, J.W., 1990. The influence of Precambrian source components on the U–Pb zircon age of a Paleozoic granite from northern Victoria Land, Antarctica. Precambrian Research 46, 275–293.

Boschetti, F., Horowitz, F.G., Hornby, P., 1999. Ambiguity analysis and the constrained inversion of potential field data, Research Review; CSIRO Exploration and Mining 1999.

Brock, D., 2003. Metamorphic constraints on the evolution of the southern Delamerian Orogen, south Australia. Unpublished B.Sc (Hons) Thesis, University of Adelaide.

Clark, D.A., 1997. Magnetic petrophysics and magnetic petrology: aids to geological interpretation of magnetic surveys. AGSO Journal of Australian Geology and Geophysics 17, 83–103.

Clarke, G.L., Powell, R., 1989. Basement–cover interaction in the Adelaide Foldbelt. Tectonophysics 158, 209–226.

Cooper, J.A., Jenkins, R.J., Compston, W., Williams, I.S., 1992. Ion-probe zircon dating of a mid-Early Cambrian tuff in South Australia. Journal of the Geological Society, London 149, 185–192.

Crawford, A.J., Cayley, R.A., Taylor, D.H., Morand, V.J., Gray, C.M., Kemp, A.I.S., Wohlt, K.E., Vandenberg, A.H.M., Moore, D.H., Maher, S., Direen, N.G., Edwards, J., Donaghy, A.G., Anderson, J.A., Black, L.P., 2003. Chapter 3. Neoproterozoic and Cambrian continental rifting, continent-arc collision and post collisional magmatism, in Birch, W.D., ed., Geology of Victoria, Volume 22: Geological Society of Australia Special Publication: Melbourne, pp. 73–93

Dahlstrom, C.D.A., 1969. Balanced cross-sections. Canadian Journal of Earth Sciences 6, 743–757.

De Paor, D.G., 1988. Balanced section in thrust belts, Part 1: construction. American Association of Petroleum Geologists Bulletin 72, 73–90.

Direen, N.G., 1998. The Palaeozoic Koonenberry fold and thrust belt, western NSW: a case study in applied gravity and magnetic modelling. Exploration Geophysics 29, 330–339.

Direen, N.G., Crawford, A.J., 2003. The Tasman Line: what is it, where is it, and is it Australia's Rodinian break-up boundary? Australian Journal of Earth Sciences 50, 491–502.

Direen, N.G., Leaman, D.E., 1997. Geophysical modelling of structure and tectonostratigraphic history of the Longford Basin, northern Tasmania. Exploration Geophysics 28, 29–33.

Direen, N.G., Lyons, P., 2002. Geophysical interpretation of the Olympic Cu–Au province, 1:250 000 scale map. Geoscience Australia, Canberra.

Direen, N.G., Lyons, P., Korsch, R.J., Glen, R.A., 2001. Integrated geophysical appraisal of crustal architecture in the eastern Lachlan Orogen. Exploration Geophysics 32, 252–262.

Dutta, S., Chatterjee, S.M., 1998. Optimization of spread configuration for seismic data acquisition through numerical modeling in tectonically complex areas; a case study from Badarpur Anticline, Cachar, India. Journal of Applied Geophysics 40, 205–222.

Dymoke, P., Sandiford, M., 1992. Phase relations of Buchan facies series pelitic assemblages: calculations and application to the Mount Lofty Ranges, South Australia. Contributions to Mineralogy and Petrology 110, 121–132.

Earth Resource Mapping Pty. Ltd, 2002. ERMapper v.6.0.

Elliott, D., 1983. The construction of balanced cross-sections. Journal of Structural Geology 5, 101.

Encom Technology, 2002. ModelVision Pro v.4.0.22. Encom Technology, Sydney, Australia.

Flöttmann, T., James, P.R., 1997. Influence of basin architecture on the style of inversion and fold-thrust belt tectonics—the southern Adelaide Fold-Thrust Belt, South Australia. Journal of Structural Geology 17, 1093–1110.

Flöttmann, T., Kleinschmidt, G., 1991. Opposite thrust systems in northern Victoria Land, Antarctica: imprints of Gondwana's Paleozoic accretion. Geology 19, 45–47.

Flöttmann, T., Oliver, R., 1994. Review of Precambrian–Paleozoic relationships at the craton margins of southeastern Australia and adjacent Antarctica. Precambrian Research 69, 293–306.

Flöttmann, T., Gibson, G.M., Kleinschmidt, G., 1993a. Structural continuity of the Ross and Delamerian orogens of Antarctica and Australia along the margin of the paleo-Pacific. Geology 21, 319–322.

Flöttmann, T., Kleinschmidt, G., Funk, T., 1993b. Thrust patterns of the Ross/Delamerian orogens in northern Victoria Land (Antarctica) and southeastern Australia and their implications for Gondwana reconstructions. In: Findlay, R.H., Unrug, R., Banks, M.R., Veevers, J.J. (Eds.), Gondwana Eight. A.A. Balkema, Rotterdam, pp. 131–139.

Flöttmann, T., James, P.R., Rogers, J., Johnson, T., 1994. Early Paleozoic foreland thrusting and basin reactivation at the Paleo-Pacific margin of the southeastern Australian Precambrian Craton: a reappraisal of the structural evolution of the southern Adelaide Fold-Thrust Belt. Tectonophysics 234, 95–116.

Flöttmann, T., James, P.R., Menpes, R., Cesare, P., Twining, M., Fairclough, M., Randabel, J., Marshak, S., 1995. The structure of Kangaroo Island, South Australia: a strain and kinematic partitioning during Delamerian basin and platform reactivation. Australian Journal of Earth Sciences 42, 35–49.

Flöttmann, T., Haines, P., Jago, J., James, P.R., Belperio, A., Gum, J., 1998.

Formation and reactivation of the Cambrian Kanmantoo Trough, SE Australia: implications for early Paleozoic tectonics at eastern Gondwana's plate margin. Journal of the Geological Society, London 155, 525–539.

Foden, J., Elburg, M.A., Turner, S.P., Sandiford, M., O'Callaghan, J., Mitchell, S., 2002. Granite production in the Delamerian Orogen, South Australia. Journal of the Geological Society, London 159, 557–575.

Foster, M.S., Price, S.J., Hill, G.S., Duque, C., Ellis, D., Stephenson, R.W., 1998. A breakthrough in the quality of seismic data from the fold belt of Papua New Guinea. The Leading Edge 17, 611–620.

Gibbs, A.D., 1983. Balanced cross-section construction from seismic sections in areas of extensional tectonics. Journal of Structural Geology 5, 153–160.

Goodge, J.W., Borg, S.C., Smith, B.K., Bennett, V.C., 1991. Tectonic significance of Proterozoic ductile shortening and translation along the Antarctic margin of Gondwana. Earth and Planetary Science Letters 102, 58–70.

Goodge, J.W., Walker, N.W., Hansen, V.L., 1993. Neoproterozoic–Cambrian basement-involved orogenesis within the Antarctic margin of Gondwana. Geology 21, 37–40.

Goscombe, B., Hand, M., Gray, D., 2003. Structure of the Kaoko Belt, Namibia: progressive evolution of a classic transpressional orogen. Journal of Structural Geology 25, 1049–1081.

Gum, J.C., 1998. The sedimentology, sequence stratigraphy and mineralization of the Silverton Subgroup, South Australia. PhD thesis, University of South Australia.

Hardage, B.A., Pendleton, V.M., Major, R.P., Asquith, G.B., Schultz, E.D., Lancaster, D.E., 1999. Using petrophysics and cross-section balancing to interpret complex structure in a limited-quality 3-D seismic image. Geophysics 64, 1760–1773.

Jago, J.B., Gum, J.C., Burtt, A.C., Haines, P.W., 2003. Stratigraphy of the Kanmantoo Group: a critical element of the Adelaide Fold Belt and the Paleo-Pacific plate margin, Eastern Gondwana. Australian Journal of Earth Sciences 50, 343–363.

Jenkins, R.J.F., 1990. The Adelaide Fold Belt: Tectonic reappraisal. In: Jago, J.B., Moore, P.S. (Eds.), The evolution of a Late Precambrian–Early Paleozoic rift complex: The Adelaide Geosyncline. Geological Society of Australia, Special Publication, vol. 16, pp. 396–420.

Jenkins, R.J.F., Sandiford, M., 1992. Observations on the tectonic evolution of the southern Adelaide Fold Belt. Tectonophysics 214, 27–36.

Jessell, M.W., Valenta, R.K., 1996. Structural geophysics; integrated structural and geophysical modeling. In: De Paor, D.G. (Ed.), Structural Geology and Personal Computers Computer Methods in the Geosciences 15, pp. 303–324.

Jones, L.E.A., Johnstone, D.W., 2001. Acquisition and processing of the 1997 Eastern Lachlan (L146) and Lachlan (L151) seismic reflection surveys. Australian Geological Survey Organisation Record 2001/09, 26–35.

Jones, P.B., 1988. Balanced cross-sections; an aid to structural interpretation. Geophysics: The Leading Edge of Exploration 7, 29–31.

Klootwijk, C.T., 1980. Early Paleozoic paleomagnetism in Australia. Tectonophysics 64, 249–332.

Leaman, D.E., 1997. Application of magnetic methods to deep basin structures. Exploration Geophysics 28, 97–105.

Lee, T.J., 1980. Rapid computation of magnetic anomalies with demagnetization included, for arbitrarily shaped magnetic bodies. Geophysical Journal of the Royal Astronomical Society 60, 67–75.

Mancktelow, N.S., 1990. The structure of the southern Adelaide Fold Belt, South Australia. In: Jago, J.B., Moore, P.S. (Eds.), The Evolution of a Late Precambrian–Early Paleozoic Rift Complex: The Adelaide Geosyncline. Geological Society of Australia, Special Publication, vol. 16, pp. 369–395.

Marshak, S., Flöttmann, T., 1996. Structure and origin of the Fleurieu and Nackara Arcs in the Adelaide fold-thrust belt, South Australia: salient and recess development in the Delamerian Orogen. Journal of Structural Geology 18, 891–908.

Marshak, S., Woodward, N., 1988. Introduction to cross-section balancing. In: Marshak, S., Mitra, G. (Eds.), Basic Methods of Structural Geology, Part II. Prentice-Hall, Englewood Cliffs, pp. 303–332.

McLean, M.A., Betts, P.G., 2003. Geophysical constraints of shear zones and geometry of the Hiltaba Suite granites in the western Gawler Craton, Australia. Australian Journal of Earth Sciences 50, 525–541.

Minty, B.R.S., Milligan, P.R., Luyendyk, A.P.J., Mackey, T., 2003. Merging airborne magnetic surveys into continental-scale compilations. Geophysics 68, 988–995.

Mitra, S., 2002. Structural models of faulted detachment folds. AAPG Bulletin 86, 1673–1694.

Morgan, J.K., Karig, D.E., 1995. Kinematics and a balanced and restored cross-section across the toe of the eastern Nankai accretionary prism. Journal of Structural Geology 17, 31–45.

Morley, C.K., 1988. Out-of-sequence-thrusts. Tectonics 7, 539–561.

Offler, R., Fleming, P.D., 1968. A synthesis of folding and metamorphism in the Mt Lofty Ranges, South Australia. Journal of the Geological Society of Australia 15, 245–266.

Oliver, R., Cooper, A.J., Truelove, A.J., 1983. Petrology and zircon geochronology of Herring Island and Commonwealth Bay and evidence for Gondwana reconstructions. In: Oliver, R. et al. (Ed.), Antarctic Earth Science. Cambridge University Press, pp. 64–68.

Paul, E.G., 1998. The geometry and controls on basement-involved deformation in the Adelaide Fold Belt, South Australia. PhD thesis, University of Adelaide.

Paul, M.K., Datta, S., Banerjee, B., 1966. Direct interpretation of two dimensional structural faults from gravity data. Geophysics 31, 940–948.

Peucat, J.J., Ménot, R.P., Monnier, O., Fanning, C.M., 1999. The Terre Adélie basement in the East Antarctica Shield: geological and isotopic evidence for a major 1.7 Ga thermal event; comparision with the Gawler Craton in South Australia. Precambrian Research 94, 205–224.

Powell, C.McA., Preiss, W.V., Gatehouse, C., Krapez, B., Li, Z., 1994. South Australian record of a Rodinian epicontinental basin and its mid-Neoproterozoic break-up (700 Ma) to form the Paleo-Pacific Ocean. Tectonophysics 237, 113–140.

Power, M.R., Hill, K.C., Hoffman, N., Bernecker, T., Norvick, M.S., 2001. The structural and tectonic evolution of the Gippsland Basin; results from 2D section balancing and 3D structural modelling. In: Hill, K.C., Bernecker, T. (Eds.), Eastern Australasian Basins Symposium 2001; A Refocused Energy Perspective for the Future. Petroleum Exploration Society of Australia, Sydney, N.S.W., Australia.

Preiss, W.V., 1987. The Adelaide Geosyncline–late Proterozoic stratigraphy, sedimentation, paleontology and tectonics. Geological Survey of South Australia Bulletin 53, 438.

Preiss, W.V., 1995a. Delamerian Orogeny. In: Drexel, J.F., Preiss, W.V. (Eds.), The Geology of South Australia. Volume 2: The Phanerozoic South Australian Geological Survey, Bulletin, vol. 54, pp. 481–495.

Preiss, W.V., 1995b. Rb/Sr dating of differentiated cleavage from the upper Adelaidean metasedimentary rocks at Hallett Cove, southern Adelaide fold belt; discussion and reply. Journal of Structural Geology. 17, 1797–1800.

Preiss, W.V., 1997. Revision of lithostratigraphy and structure, and evidence of volcanism in Lower Burra Group type sections, Carey-Gully-Basket Range area, Mount Lofty Ranges. MESA Journal 7, 37–46.

Preiss, W.V., 2000. The Adelaide Geosyncline of South Australia and its significance in Neoproterozoic continental reconstruction. Precambrian Research 100, 21–63.

Preiss, W.V., 2003. Compiler—Geology map sheets 1:100 000 ADELAIDE, MILANG. Geological Survey of South Australia, Department of Primary Industries and Resources, South Australia.

Rajagopalan, S., 1989. Aeromagnetic interpretation of the Kanmantoo Group, South Australia. PhD thesis, University of Adelaide.

Rowan, M.G., Kligfield, R., 1989. Cross section restoration and balancing as aid to seismic interpretation in extensional terranes. AAPG Bulletin 73, 955–966.

Sayers, J., Symonds, P.A., Direen, N.G., Bernardel, G., 2001. Nature of the continent–ocean transition on the non-volcanic rifted margin of the central Great Australian Bight. In: Wilson, R.C.L., Whitmarsh, R.B., Taylor, B., Froitzheim, N. (Eds.), Non-volcanic Rifting of Continental Margins; A Comparison of Evidence from Land and Sea Geological Society (London) Special Publication 187, pp. 51–76.

Schlinger, C.M., 1985. Magnetization of lower crust and interpretation of regional magnetic anomalies: example from Lofoten and Vesterålen, Norway. Journal of Geophysical Research 90, 11484–11504.

Sheraton, J.W., Tingey, R.J., Black, L.P., Oliver, R.L., 1993. Geology of the Bunger Hills area, Antarctica: implications for Gondwana correlations. Antarctic Science 5, 85–102.

Sprigg, R.C., 1946. Reconnaissance geological survey of a portion of the western escarpment of the Mt. Lofty Ranges. Transaction of the Royal Society of South Australia 70, 313–347.

Sprigg, R.C., Wilson, B., 1954. Echunga, Geological Atlas 1 Mile Series. Geological Survey of South Australia. Department of Mines, Adelaide.

Storey, B.C., Macdonald, D.I.M., Dalziel, I.W.D., Isbell, J.L., Millar, I.L., 1996. Early Paleozoic sedimentation, magmatism, and deformation in the Pensacola Mountains, Antarctica: the significance of the Ross Orogeny. GSA Bulletin 108, 685–707.

Stump, E.J., White, A.J.R., Borg, S.G., 1986. Reconstruction of Australia and Antarctica: evidence from recent mapping. Earth and Planetary Science Letters 79, 348–360.

Von Der Borch, C.C., 1980. Evolution of late Proterozoic to early Paleozoic Adelaide Foldbelt, Australia: comparisons with post-Permian rifts and passive margins. Tectonophysics 70, 115–134.

Woodward, N.B., Boyer, S.E., Suppe, J., 1989. Balanced geological cross-sections: an essential technique in geological research and exploration, Short Course in Geology, vol. 6. American Geophysical Union.

Yassaghi, A., James, P.R., Flöttmann, T., 2000. Geometric and kinematic evolution of asymmetric ductile shear zones in thrust sheets, southern Adelaide Fold–Thrust Belt, South Australia. Journal of Structural Geology 22, 889–912.

Yassaghi, A., James, P.R., Flöttmann, T., Winsor, C.N., 2004. *P–T* conditions and kinematics of shear zones from the southern Adelaide Fold–Thrust Belt, South Australia: insights into the dynamics of a deeply eroded orogenic wedge. Australian Journal of Earth Sciences 51, 301–317.